VILNIUS UNIVERSITY
LIFE SCIENCES CENTER

Agnė Kvietkauskaitė

Metabolic Reprograming of Cancer Cells Using Riboflavin to Induce Synthetic Lethality by CAIX Inhibitors

Master's Thesis

Molecular Biotechnology study program, government code 6211FX021

Biotechnology study field

Thesis supervisor

Dr. Jurgita Matulienė

Consultant

Prof. Dr. Ramunas Martin Vabulas

Thesis completed at

Department of Biothermodynamics and Drug Design of the LSC Institute of Biosciences

Department of Systems Biochemistry of the Charité – University Medicine Berlin Institute of Biochemistry

Vilnius 2025

Contents

Abbreviations

143B – Human osteosarcoma cell line

BSA – Bovine serum albumin

CA – Carbonic anhydrase

CA9 – CAIX coding gene

CAIX – Carbonic anhydrase IX

dFBS – Dialyzed fetal bovine serum

DMEM – Dulbecco's modified Eagle medium

DMSO – Dimethyl sulfoxide

LC_{50} – Half-maximal lethal concentration

EDTA – Ethylenediaminetetraacetic acid

FACS – Fluorescence-activated cell sorting

FBS – Fetal bovine serum

HIF-1– Hypoxia-inducible factor-1

O-DMEM – DMEM without riboflavin

PBS – Phosphate buffered saline

PEI – Polyethylenimine

PFA – Paraformaldehyde

pH_e – Extracellular pH

pH_i – Intracellular pH

RF – Riboflavin

RT – Room temperature

SRB – Sulforhodamine B

TCA – Trichloroacetic acid

Tris – Tris(hydroxymethyl)-aminomethane

Opti-MEM - chemically defined, low protein, Minimal Essential Medium (MEM)

Introduction

Enzymes known as carbonic anhydrases (CA) catalyse the reversible hydration process of carbon dioxide to bicarbonate (HCO_3^-) ion and a proton (H^+). Acid-base homeostasis, calcification, carbon dioxide transport, pH and fluid balance control in the body are only a few of numerous physiological activities these enzymes support (Zamanova, Shabana, Mondal & Ilies, 2019).

Carbonic anhydrases are divided into eight families and are found in various organisms: protozoa, algae, plants, fungi, and animals. Overall, there are fifteen distinct carbonic anhydrases in humans, all of which fall within the α-CA family. Impaired CA activity has been associated with various diseases and pathological conditions including glaucoma, obesity, epilepsy, acute mountain sickness, idiopathic intracraneural hypertension, neuropathic pain, cerebral ischemia, rheumatoid arthritis, oxidative stress, Alzheimer's disease and cancer (Suppuran, 2021).

Carbonic Anhydrase IX (CAIX) is a dimeric membrane protein widely expressed in several malignancies, and in the stomach and testes of healthy persons. Mostly present on the surface of cancer cells, CAIX stimulates tumour development and spread under hypoxic conditions. Consequently, CAIX is seen as a good target for cancer diagnosis and treatment. Development of inhibitors of the CAIX activity is in progress. It is not an easy task, since the inhibitors must be effective and selective, i.e., they should not interact with other carbonic anhydrases, hence preventing undesired side effects.

In cancer cells, metabolic reprogramming is the bioenergetic shift that advances malignant transformation and tumour growth. The most famous example, a Warburg effect, is a reprogramming whereby cancer cells switch to glycolysis as manifested by the rise of glucose absorption and lactate generation. Scientists want to exploit this naturally occurring metabolic transformation of cancer cells for therapeutic purposes. For example, strategies using the glucose analogue galactose and the vitamin riboflavin (RF) have been investigated to weaken cancer cells by disrupting their metabolism. The lack of RF alters the stability and activity of the respiratory complexes of complex I and II in the mitochondria, which makes cancer cells dependent on glycolysis as source of energy. On the other hand, galactose is known to suppress glycolysis in favour of the mitochondrial oxidative phosphorylation. Combination of these approaches might provide a novel strategy that, by changing cellular energy metabolism, might influence cancer cell viability and thus improve therapy outcomes.

The aim of the project:

Sensitize tumours against CAIX inhibitors by means of the metabolic reprogramming of tumour cells and identify the inhibitor-driven changes.

Objectives of the thesis:

1. Set up the experimental model:
   - 1.1. Establish flow cytometry measurements to determine conditions for metabolic reprogramming;
   - 1.2. Establish measurements of mitochondrial respiration by the Seahorse assay;
   - 1.3. Determine effective inhibitor concentrations.
2. Quantify the effects of two CAIX inhibitors (VD11-4-2 and AZ19-3-2):
   - 2.1. Using CRISPR/Cas9, establish CA9 gene knockout cancer cell lines;
   - 2.2. Use the Seahorse assay to quantify the effect of the inhibitors on the mitochondrial respiration;
   - 2.3. Use flow cytometry to quantify the effects of the inhibitors on cellular viability.
3. Proteomic characterization of the changes in expression of oncoproteins:
   - 3.1. Protein expression analysis of wild-type cell lines grown in different conditions.

1. Literature review

1.1. Carbonic anhydrases

Carbonic anhydrases (CA, EC 4.2.1.1) are metalloenzymes classified under the lyase class, catalysing the reversible hydration of carbon dioxide (CO2):

$$CO_2 + H_2O \rightleftharpoons H_2CO_3 \rightleftharpoons HCO_3^- + H^+$$

The spontaneous hydration of CO2 occurs at a rate insufficient to meet the metabolic demand for CO_2 and HCO_3–, both being crucial for organisms to grow, reproduce, maintain structure, and respond to environmental changes. Various CA enzymes can accelerate the CO_2 hydration reaction up to a one million times compared to the uncatalysed reaction (Baranauskienė & Matulis, 2019a).

CA enzymes have been studied for decades and are grouped to enzyme superfamily. The superfamily comprises eight distinct families or classes denoted by Greek letters: alpha (α), beta (β), gamma (γ), delta (δ), zeta (ζ), eta (η), theta (θ), and iota (ι). While structurally distinct across different classes, the CAs catalyse the same reaction in various organisms. Alpha (α)-CA is found in animals, plant cytoplasm, algae, and gram-negative bacteria. Beta (β)-CA is present in bacteria, plant chloroplasts, fungi, and archaea. Gamma (γ)-CA occurs in bacteria, cyanobacteria, and archaea. Delta (δ), zeta (ζ), and theta (θ)-CA are found in marine diatoms, while eta (η)-CA is present in algae (Baranauskienė & Matulis, 2019a; Jensen et al., 2019). Recently discovered iota (ι)-CA is found in marine phytoplankton *Thalassiosira pseudonana* and bacteria *Burkholderia territorii* (Nocentini, Supuran & Capasso, 2021).

As mentioned above, CAs are metalloenzymes with a metal ion cofactor at the active site, which is essential for their catalytic activity. Typically, this cofactor is a zinc ion (Zn^{2+}), coordinated by three amino acid residues, but other ions like cobalt (Co^{2+}), cadmium (Cd^{2+}), manganese (Mn^{2+}), and iron (Fe^{2+}) can also be found (Baranauskienė & Matulis, 2019a; Jensen et al., 2019; Nocentini et al., 2021).

1.1.1. Human Carbonic Anhydrases

In humans, there are a total of 14 CA isoforms, which are structurally very similar to each other. All of them belong to the α-CA family. However, only twelve isoforms are catalytically active. The active enzymes differ in their cellular and organismal localization, catalytic activity strength, and pathologies associated with their defects (Table 1). The remaining three carbonic anhydrases are catalytically inactive and are also known as carbonic anhydrase-related proteins. Carbonic anhydrase-related proteins have lost their catalytic function due to mutations in the amino acid residues coordinating the metal ion cofactor at the active site (histidine was replaced by other amino acids). Consequently, they lack zinc ion at the active site and cannot perform the carbon dioxide hydration (Chegwidden, 2021).

The localization of human carbonic anhydrases within cells varies. Five carbonic anhydrase isoforms (CAI, II, III, VII, and XIII) and the catalytically inactive carbonic anhydrases (CARP VIII, X, XI) are found in the cytosol. Two isoforms (CAVA and VB) are located in mitochondria. Additionally, one membrane-associated isoform (CAIV) and three transmembrane proteins (CAIX, XII, and XIV) are present in cells, all of whose catalytic domains are oriented towards the extracellular space. Only CAVI is secreted from the cell. All CA isoforms are monomers, except for three - CAVI, IX, and XII - which are dimeric in structure (Figure 1).

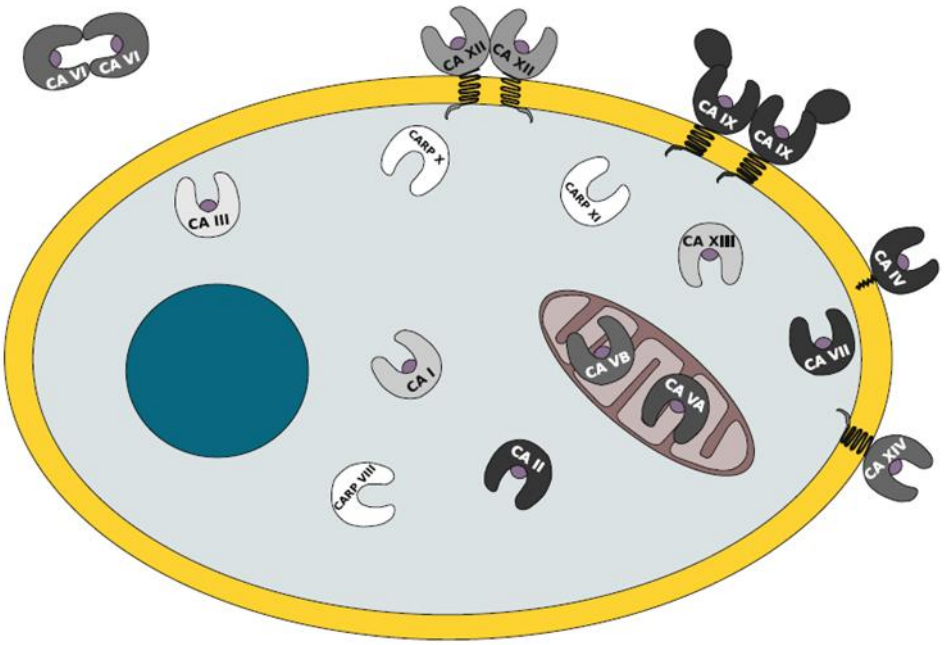

Figure 1. Localization of different CA isoforms in the cell. Horseshoes represent the enzymes; the intensity of the shade indicates their relative catalytic activity. Zink ions are represented by purple sphere. (Baranauskienė & Matulis, 2019a.)

The α-CA catalysed reaction occurs via a two-step ping-pong mechanism. In the first step (Figure 2A and B), a hydroxide group bond to the zinc ion undergoes a nucleophilic attack on CO_2, forming the enzyme-HCO_3 complex (Figure 2C). Subsequently, the HCO_3^- anion is released from the active site and replaced by a water molecule (Figure 2C and D). In the second step (Figure 2D and A), which limits the rate of the reaction, the catalytically active zinc ion is regenerated with a coordinated hydroxide group, deprotonating the water molecule attached to the zinc ion. The proton is carried away with the assistance of a buffer solution. In some CAs, the proton is transferred onto the His64 residue, which acts as a proton shuttle, directly transferring the proton from the water molecule to the outside (Silverman & Lindskog, 1988; Baranauskienė & Matulis, 2019b; Angeli, Carta & Supuran, 2020).

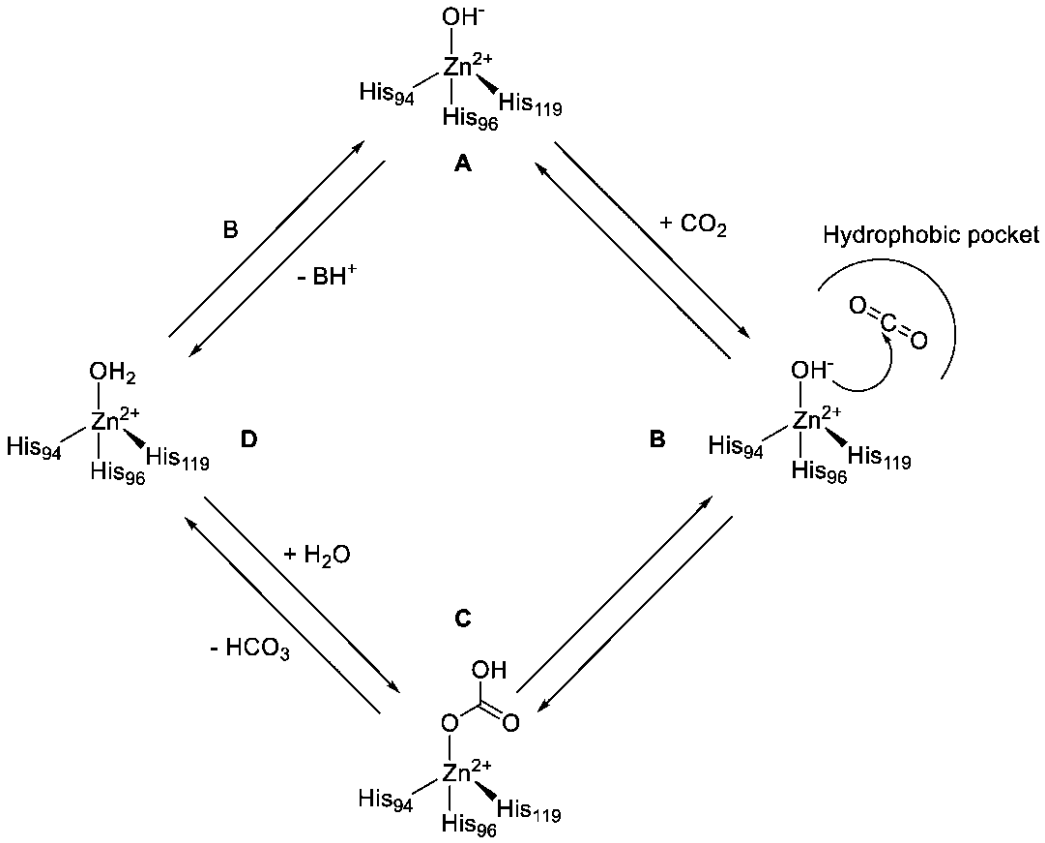

Figure 2. Mechanism of CO_2 hydration reaction catalysed by α-CA. (Angeli, Carta & Supuran, 2020).

CAs participate in numerous essential physiological processes, including transport of H+, CO2, ions, and water, maintenance of acid-base homeostasis, pH regulation, and fluid balance in the body (Zamanova et al., 2019; Chegwidden, 2021). Due to their wide spectrum of functions, CA isoforms, when mutated, are involved in many diseases and disorders. CAI, II, IV, and XII isoforms are associated with glaucoma (Maren, 1987; Stoner et al., 2022), CAII, VII, and XIV with epilepsy (Ciccone et al., 2021; Zavala-Tecuapetla et al., 2020), and CAIII and IV with oxidative stress (Shaikh et al., 2020; di Fiore et al., 2018). Additionally, there is an association between obesity and impaired expression of CAVA and CAVB (Supuran, 2022). Cancer-related diseases, currently receiving significant attention, are linked to CAIX and CAXII isoforms (Pastorekova & Gillies, 2019; Koltai et al., 2020).

Table 1. Activity, localizations, related diseases and disorders of human CA isoforms

CA isoform	Catalytic activity	Localization in the cell	Localization in the human body	Related diseases and disorders
CAI	Average	Cytosol	Red blood cells, digestive tract, eyes	Bipolar disorder, glaucoma, edema
CAII	High	Cytosol	Red blood cells, digestive tract, eyes, osteoclasts, kidneys, lungs, testes, brain	Edema, high-altitude sickness, glaucoma, Alzheimer's disease, epilepsy, sleep apnea
CAIII	Low	Cytosol	Skeletal muscles, adipocytes	Oxidative stress, myasthenia gravis
CAIV	High	Membrane	Kidneys, lungs, pancreas, eyes, brain, blood vessel capillaries, rectum, heart muscle	Glaucoma, LOPL (Low-Pressure Open-Angle Glaucoma), retinitis pigmentosa, stroke
CAVA	Average	Mitochondria	Liver	Obesity
CAVB	High	Mitochondria	Heart and skeletal muscles, pancreas, kidneys, digestive tract, spinal cord	Obesity
CAVI	Average	Secreted	Salivary and mammary glands	Tooth decay
CAVII	High	Cytosol	Central nervous system	Epilepsy, neuropathic pain, oxidative stress
CAIX	High	Transmembrane	Tumours, gastrointestinal epithelium, testes	Cancer
CAXII	Average	Transmembrane	Kidney, intestinal, and reproductive organ epithelium, eyes, tumours	Glaucoma, cancer
CAXIII	Average	Cytosol	Kidneys, brain, lungs, digestive tract, reproductive organs	Infertility
CAXIV	Average	Transmembrane	Kidneys, brain, liver, heart	Epilepsy, retinopathy

Sources: Chegwidden, 2021; Baranauskienė & Matulis, 2019.

1.1.2. Carbonic anhydrase IX

Carbonic anhydrase IX (CAIX) is a transmembrane metalloenzyme containing a zinc ion and belonging to the α-CA family. CAIX was discovered in 1992 upon observing its expression in HeLa cells (human cervical adenocarcinoma). This molecule was initially named "MN protein" (Pastoreková, Závadová, Košťál, Babušíková, & Závada, 1992; later, Pastorek et al. (1994)). However, the characterization of the CA9 gene and identification of the CA activity, led to the reclassification of "MN protein" as CAIX.

Mature CAIX consists of a N-terminal proteoglycan-like domain (PG), a CA catalytic domain, a transmembrane helix (TM) and a short intracellular tail (IC) at the C-terminus (Figure 3). The PG domain is unique to CAIX and supports cell adhesion and intercellular connections. Within the intracellular tail (IC), which controls CAIX catalytic activity and is related to signal transduction, there are three main phosphorylation sites: Thr443, Ser448, and Tyr449. Protein kinase A (PKA) activates CAIX by phosphorylating Thr443 and a phosphatase dephosphorylating Ser448. Tyr449 participates in the epidermal growth factor/epidermal growth factor receptor (EGF/EGFR) and phosphatidylinositol-3 kinase/Akt kinase (PI-3K/Akt) signal transduction pathway (Queen, Bhutto, Yousuf, Syed, & Hassan, 2022). Phosphorylation likely affects the spatial structure of the catalytic domain, thereby enhancing its activity.

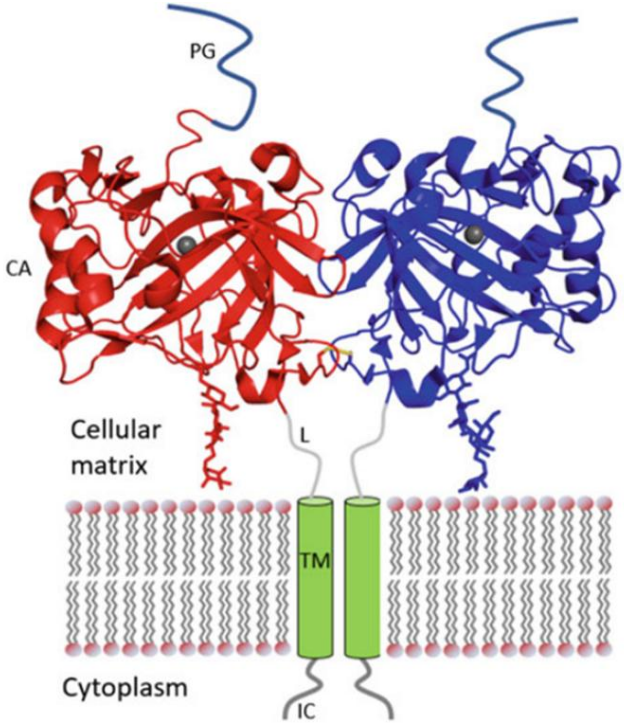

Figure 3. The structure of matured CAIX. Proteoglycan-like domain (PG), catalytic domain (CAIX crystal structure PDB ID: 3IAI), linker region (L), transmembrane helix (TM) and intracytoplasmic tail (IC). (Tars and Matulis, 2019)

Crystallographic studies have revealed that the catalytic domain of CAIX (Figure 4) is a compact globular domain. Its structure closely resembles other α-CA enzymes. The domain consists of an

α-β-α sandwich fold, where a β-sheet formed by ten anti-parallel β-strands constitutes the core of the protein (Alterio et al., 2009; Tars & Matulis, 2019). Two catalytic domains in the dimer are linked and stabilized by a single intermolecular disulfide bond. The main function of CAIX protein is pH regulation.

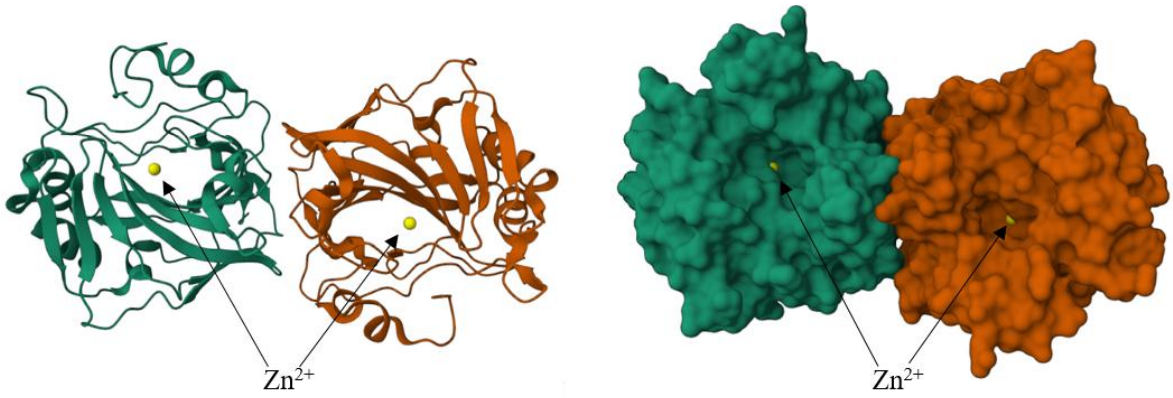

Figure 4. CAIX catalytic domain (PDB ID: 3IAI). Two CAIX monomers are represented in different colours. Zink ions (yellow sphere) in the active site are indicated by the arrows. (Alterio et al., 2009)

In healthy individuals, CAIX is predominantly expressed in the stomach and testes. However, its increased expression is observed in many cancerous tumours, such as kidney, lung, cervical, ovarian, oesophageal, and breast carcinomas. Overexpression of CAIX is particularly noted in hypoxic regions of tumours and is associated with the activation of hypoxia-inducible factor-1 (HIF-1). Additionally, CAIX can be detected in less hypoxic or even normoxic areas, as its expression can also be activated by the mitogen-activated protein kinase (MAPK) pathway (Becker, 2020).

CAIX plays a significant role in regulating intracellular pH (pH_i) and extracellular pH (pH_e), thereby inducing extracellular acidosis, which influences cancer cell migration and invasion, promoting metastasis formation and correlating with poor disease prognosis. Evidence supporting close association of CAIX with cancer development and survival includes studies demonstrating that its knockdown, the pharmacological inhibition of enzymatic activity, or overexpression of catalytically inactive CAIX mutants reduce cancer cell migration and metastasis (Becker & Deitmer, 2020).

CAIX catalyses the reversible hydration of CO_2 in the extracellular space, allowing it to regulate both pH_i and pH_e. This prevents the accumulation of high CO_2 concentrations close to the plasma membrane, facilitating CO_2 removal from the cell and resulting in acidic pH_e and alkaline pH_i (Becker, 2020). While an acidic microenvironment promotes tumour progression, pH_e should not be too low to avoid acidification-induced necrosis of cancer cells. Unlike other CA isoforms, CAIX is most active around pH 6.8, a value close to tumour pHe. When pH exceeds 6.8, the hydration reaction (H^+ formation) is faster than the dehydration reaction, leading to extracellular acidification. Conversely, when pH drops below 6.8, CAIX removes H^+ by means of dehydration reaction, preventing

further acidification. Lee et al. (2018) demonstrated that CAIX not only contributes to extracellular acidification but also stabilizes pH_e at a moderately acidic level in spheroids and tumour xenografts. This moderate acidity is well-tolerated by cancer cells but can be lethal to normal cells, suggesting that maintaining a stable acidic pH_e may be an evolutionary strategy of cancer cells to create an environment conducive to tumour growth and invasion (Becker, 2020).

In summary, CAIX protects tumour cells from extracellular acidosis and impacts cancer cell migration and invasion through both catalytic and non-catalytic mechanisms, promoting metastasis and correlating with poor disease prognosis. For these reasons, CAIX inhibitors are being developed for cancer therapy and diagnostics.

1.2. Carbonic anhydrase inhibitors

CA inhibitors are compounds that inhibit the CO_2 hydration reaction catalysed by CAs. For this reason, they are used to mitigate or eliminate the effects of diseases and disorders discussed in previous sections on the human body. One of the most important aspects of drug development is ensuring specificity to a target protein. Inhibitors must interact not only strongly, but also specifically with the target CA. Interaction with other CAs should be minimal or non-existent to avoid side effects.

Based on their binding characteristics with CA, inhibitors can be divided into two major groups (Baranauskienė & Matulis, 2019a). The first group includes compounds that bind to zinc ion, such as primary sulfonamides, sulfamates, sulfamides, carboxylates, hydroxamates, dithiocarbamates, xanthenes, and phosphonates. The other group consists of compounds that do not directly bind with the zinc ion. This group includes phenols, polyamines, certain carboxylates, sulfocoumarins, and 2-thioxocoumarins, which bind to the water molecule or hydroxyl group associated with the zinc ion. Additionally, this group includes compounds that block substrate entry into the active site, such as coumarins and fullerenes, as well as inhibitors that bind near the active site and inhibit by blocking His64, which functions as a proton shuttle.

Classic CA inhibitors are primary sulfonamides and sulfamates, over 10 of them are approved by the FDA for the treatment of glaucoma, epilepsy, high-altitude sickness, cerebral edema, and seizures (Figure 5). Two sulfonamides are currently being investigated in clinical trials (such as SLC-0111, E7070) for breast cancer treatment.

The main challenge in developing CA inhibitors is their selectivity. Their selectivity is determined by the physical properties of inhibitors (size, structure, hydrophobicity/hydrophilicity, etc.) and the structural differences between CA isoforms. CA proteins are very similar in structure, with relatively small sequence differences between isoforms, especially among amino acids in the active site. Additionally, all carbonic anhydrases have an almost identical catalytic domain structure, composed of α-helices and β-sheets, resulting in similar-sized active site cavities. However, CAIX stands

out because its active site is wider compared to other CAs, allowing it to accommodate ligands with larger substituents (Zakšauskas et al., 2021). This feature can be exploited to develop CAIX-selective inhibitors.

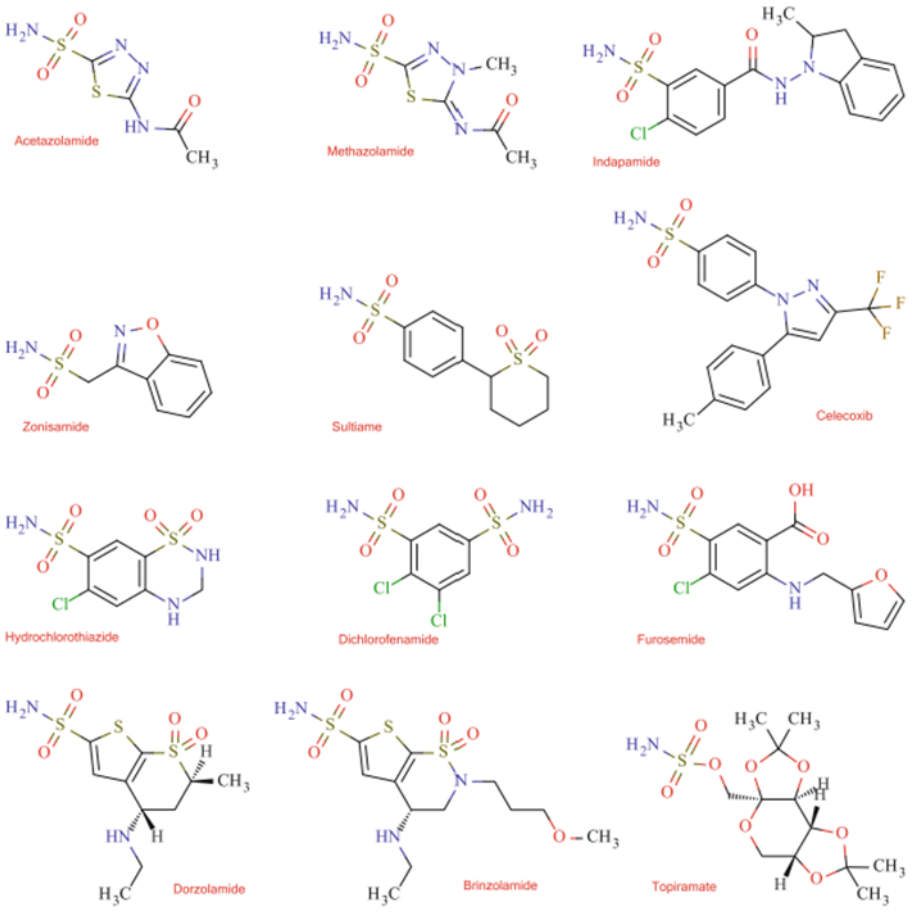

Figure 5. Examples of some most popular drugs with the CA-inhibiting activity. (Baranauskienė & Matulis, 2019a)

Inhibitors used in this work, VD11-4-2 and AZ19-3-2 (Figure 6), were synthesized at Vilnius University, Department of Biothermodynamics and Drug Design (DBDD). Both inhibitors are selective CAIX inhibitors (Table 2). The synthesis and properties of VD11-4-2 are described in the article by Dudutienė *et. al.* (2014), of AZ19-3-2 – in the article by Petrosiute *et. al.* (2024).

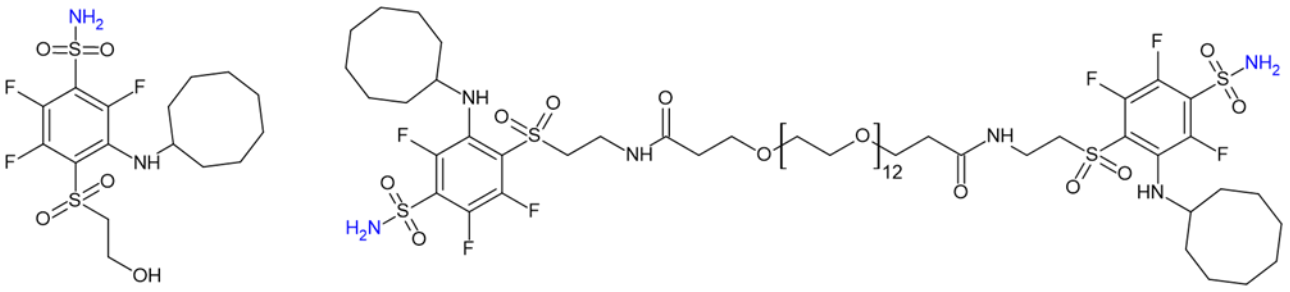

VD11-4-2 AZ19-3-2

Figure 6. Chemical structures of CAIX inhibitors used in this work

Table 2. Dissociation constants of compound binding to recombinant prepared and affinity-purified catalytically active human CA isozymes as obtained TSA at 37 °C.

	K_d (nM)											
	CAI	**CAII**	**CAIII**	**CAIV**	**CAVA**	**CAVB**	**CAVI**	**CAVII**	***CAIX***	**CAXII**	**CAXIII**	**CAXIV**
VD11-4-2	830	56	34000	61	3300	16	67	8.6	***0.032***	2.9	4.0	4.3
AZ19-3-2	2400	81	>DL	390	3000	28	50	280	***0.025***	16	11	33

>DL – the Kd value is above the detection limit (DL) of 200 000 nM

1.3. Metabolic reprograming of cancerous cells

In cancer cells, metabolic reprogramming describes bioenergetic alterations that help cancer cells to adapt their metabolism to challenging growth conditions, therefore supporting malignant transformation and tumour development (Navarro et al., 2022). Because they divide and multiply constantly, cancer cells consume more energy than ordinary cells. Tumour cells require a lot of nutrients and energy if they are to grow and spread. The upregulation of glycolysis despite normoxia, the so-called Warburg effect, causes a notable increase in glucose absorption and is accompanied by accumulation of lactate rather than pyruvate (Sun et al., 2019, Warburg, 1956). Researchers are looking for strategies to inhibit this naturally occurring reprogramming of cancer cells with the goal to effectively target cancer metabolism. This work investigated metabolic reprogramming techniques utilizing exchange of glucose with galactose and depletion of the vitamin riboflavin (RF) in cell culture media. These strategies are expected to disrupt energy metabolism in cancer cells. In the mitochondria, RF shortage reduces the activity of the respiratory complexes I and II, therefore forcing cancer cells to rely largely on glycolysis for ATP synthesis (Mosegaard et al, 2020). Galactose, in contrast, makes cells dependent more on mitochondrial oxidative phosphorylation. These approaches were supposed to shed light on how changing cellular energy metabolism might affect cancer cell activity and enhance the effects of simultaneous treatments with inhibitors against CAIX.

1.3.1. Metabolic reprogramming with riboflavin

Using RF, also known as vitamin B2, a vital component in cellular redox processes, is one of the new approaches to change cancer metabolism. Flavoproteins are involved in several metabolic processes including mitochondrial oxidative phosphorylation, the tricarboxylic acid (TCA) cycle, and fatty acid oxidation and depend critically on riboflavin-derived cofactors flavin mononucleotide (FMN) and flavin adenine dinucleotide (FAD) (Mosegaard et al, 2020). RF depletion might possibly change the metabolic condition of cancer cells by inactivating these pathways, therefore influencing proliferation and survival of affected cells.

Transformed into its active forms, FMN and FAD, RF becomes a necessary cofactor for several oxidative enzymes (Figure 7). Effective ATP generation by oxidative phosphorylation depends on

these enzymes. Depletion of RF from growing environment of the cell makes their mitochondrial function change significantly. Lack of RF often causes a decrease in mitochondrial biogenesis and activity, therefore reducing ATP generation. Even under aerobic settings, this drop in energy generation might lead to a metabolic change toward glycolysis. Moreover, the mitochondrial membrane potential might be lowered, which would produce more reactive oxygen species (ROS) formation and oxidative stress. These mitochondrial abnormalities can cause a drop in general cellular viability and proliferation and can lead to cell death. Apart from its roles in redox balance and energy production, RF influences the metabolism of amino acids and lipids as well. Acyl-CoA dehydrogenases, which perform the second step of during fatty acid β-oxidation, are flavoproteins with FAD as the activity-determining cofactor. By helping these enzymes to oxidize fatty acids, RF enables the alternative energy source for cells and reduces lipid accumulation connected with cancer cell development (Nisco et al., 2024).

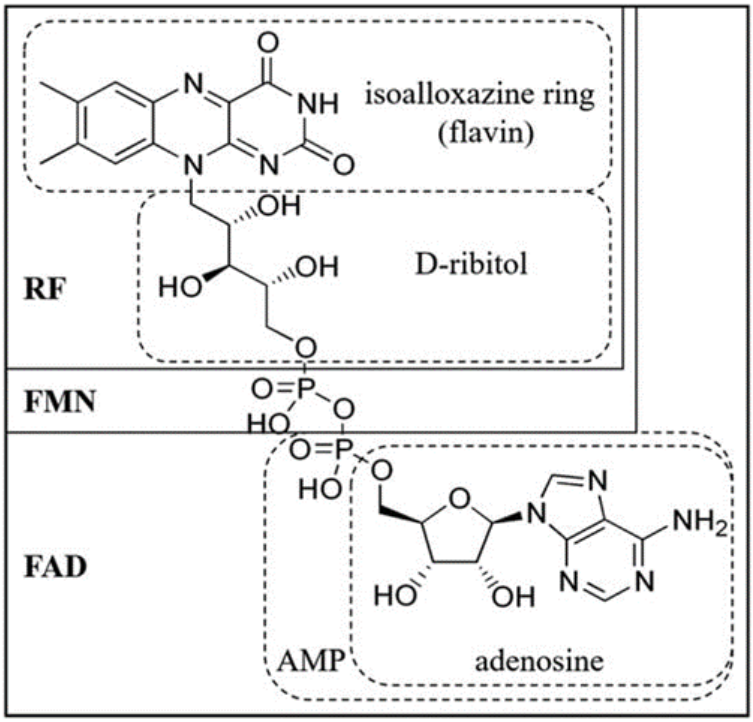

Figure 7. Chemical structure and nomenclature of flavins. RF – riboflavin; FMN – flavin mononucleotide; FAD – adenine dinucleotide; AMP – adenosine monophosphate. (Liu et al., 2020)

In summary, targeting cancer cell metabolism could be achieved by RF-mediated metabolic reprogramming. By altering important metabolic pathways, RF can lower the metabolic flexibility of cancer cells therefore increasing their sensitivity to concomitant therapeutic manipulations. Deeper understanding of the RF dependent metabolic activities and synergistic effects with other metabolic drugs could provide novel therapeutic choices in fight against cancer.

1.3.2. Metabolic reprogramming using galactose

Especially in the context of cancer biology, galactose metabolism presents another powerful possibility for metabolic reprogramming. Galactose, when supplied instead of glucose, makes cells dependent more on oxidative phosphorylation for ATP synthesis than glucose, which largely drives glycolysis and the Warburg effect in cancer cells. The Leloir pathway transforms galactose to glucose-1-phosphate (Holden, Rayment & Thoden, 2003), yet this pathway is obviously insufficient when glucose is full exchanged to galactose. Thus, galactose-burning cells generates insufficient levels of ATP via glycolysis, which drives them more toward mitochondrial oxidative phosphorylation.

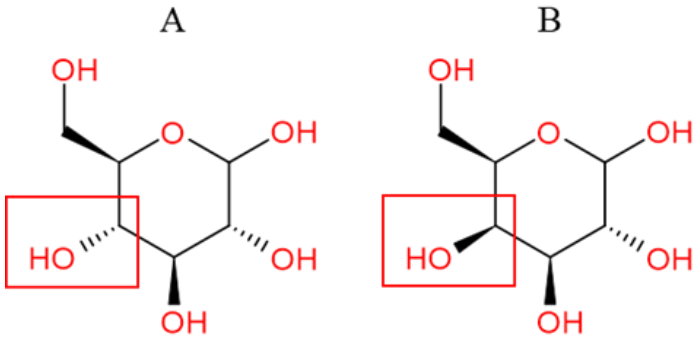

Figure 8. Structural difference between D-glucose (A) and D-galactose (B).

Indeed, cancer cells fed galactose display reduced glycolytic flux and higher mitochondrial activity. This metabolic modification in cancer cells can create therapeutically welcomed vulnerabilities. For example, cells start depending more on intact oxidative phosphorylation and thus become more sensitive to inhibitors targeting at mitochondrial activity. Therefore, using galactose as a metabolic reprogramming tool would synergize with treatments aimed at lowering mitochondrial activity and make them more efficient.

Galactose metabolism can influence other metabolic pathways as well. Reduced glycolytic flux of galactose-fed cells can affect the pentose phosphate pathway and lipid synthesis (Conte, van Buuringen, Voermans, & Lefeber. 2021). These changes can affect nucleotide and lipid availability, therefore affecting cell survival and proliferation. By changing these pathways, galactose metabolism can disrupt the anabolic flexibility of cancer cells, further raising their vulnerability to metabolic stress and therapy interventions.

The specificities of tumour metabolism enable cancer cells to sustain high proliferation and tumour formation and spread under difficult conditions. The current project aimed at elucidating how human osteosarcoma metabolism is affected by galactose and RF depletion. While galactose raises oxidative phosphorylation and reduces glycolytic activity, RF depletion increased cellular energy household reliance on glycolysis because of the mitochondrial damage. We hypothesized that these metabolic reprogramming can modify the sensitivity of cancer cells to the CAIX-targeting inhibitors.

1.4. Experimental techniques used in this work

New anticancer drugs have to be tested in *in vitro* systems before entering preclinical or clinical trials. To evaluate cellular sensitivity to novel chemicals, investigations often start with cells cultivated as monolayers. These simple models help to maximize dosing and increase the accuracy of toxicity assessments by allowing flexible screening of how cancer cells react to various dosages in different culture environments. This approach guarantees that just the most promising medication candidates go to further advanced phases of study.

1.4.1. Cell viability assays

Testing how various drugs affect the viability of cancer cells cultured as monolayers remains probably most widely used method to assess efficacy and toxicity. Cell viability tests can apply colorimetric, fluorometric, luminometric, flow cytometric, and dye exclusion methods. Colorimetric tests are rather attractive because of their simplicity. These tests use reagents which change colour in response to the cellular metabolic activity. Among these are reagents SRB, AlamarBlue, MTT, MTS, XTT, WST-1 and WST-8. A spectrophotometer is used to quantify the extent of the respective colour change and thus makes these tests simple, safe and, in most cases, cost-effective (Kamilowicz, Sari, Ozdal & Capanowicz, 2020).

AlamarBlue Assay

AlamarBlue assay is a commonly used cell viability assay which is based on the reduction of resazurin, a blue, non-toxic, cell-permeable dye (Figure 9). In live cells it is reduced to resorufin, a pink and extremely fluorescent compound The intensity of fluorescence or colour change is directly proportional to the number of living cells present in the sample. This colorimetric and fluorometric change enables quantitative measurement of cell viability and proliferation in a variety of cell types, including mammalian, bacterial, plant, and fungal cells. This assay is fast, sensitive, appropriate for high-throughput screening without harming the cells or requiring cell lysis.

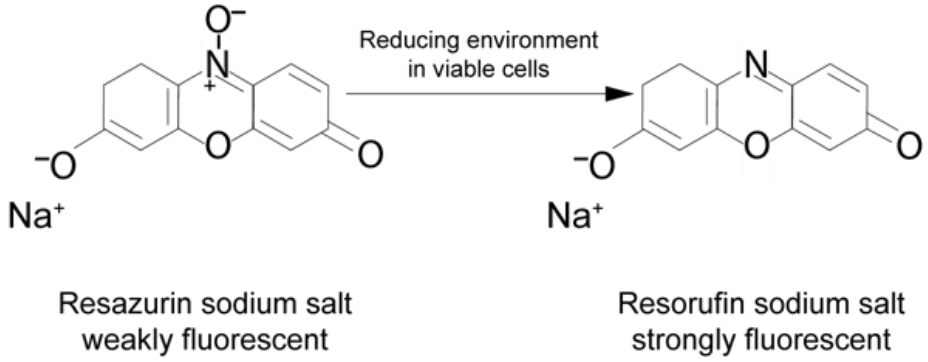

Figure 9. AlamarBlue assay principle.

SRB Assay

Sulforhodamine B (SRB) dye (Figure 10) binds to proteins and thus allows quantifying cells in a straightforward manner. The test makes use of the ability of the anionic SRB to bind amino acids of cellular proteins under mildly acidic conditions to basic. Solubilized and quantified, the bound dye provides an indirect measure of cell numbers, hence, the cell viability upon given treatment conditions. Specifically, the assay allowed quantifying the effect of CAIX inhibitors on the survival of the human osteosarcoma 143B cells and determining their respective half-maximal lethal concentrations (LC_{50}).

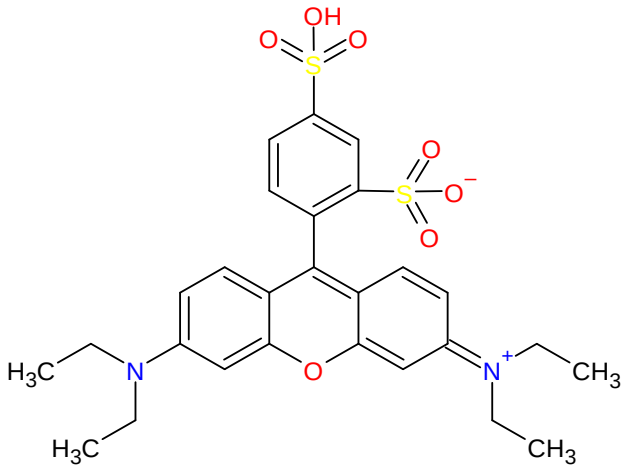

Figure 10. Structure of sulforhodamine B.

1.4.2. Seahorse assay

For assessing the metabolic activity of living cells the Seahorse XF Analyzer is commonly used. The Seahorse-generated real-time data enables researchers to address diverse metabolic functions and identify their alterations under different conditions.

Seahorse XF Analyzer monitors oxygen consumption rate (OCR) and extracellular acidification rate (ECAR) of live cells in real-time fashion. OCR and ECAR are proxies of the mitochondrial respiration and glycolytic fermentation, respectively. The so-called mitochondrial stress test is commonly used and involves application of a number of mitochondrial respiratory chain-targeting inhibitors. It allows uncovering significant aspects of mitochondrial function including baseline respiration, ATP production, proton leak, peak respiration, and spare respiratory capacity. To acquire these results, the following compounds are used in the assay: oligomycin (an inhibitor of the ATP synthase), FCCP (an uncoupling agent), and a mix of rotenone and antimycin A (inhibitors of complexes I and III, respectively).

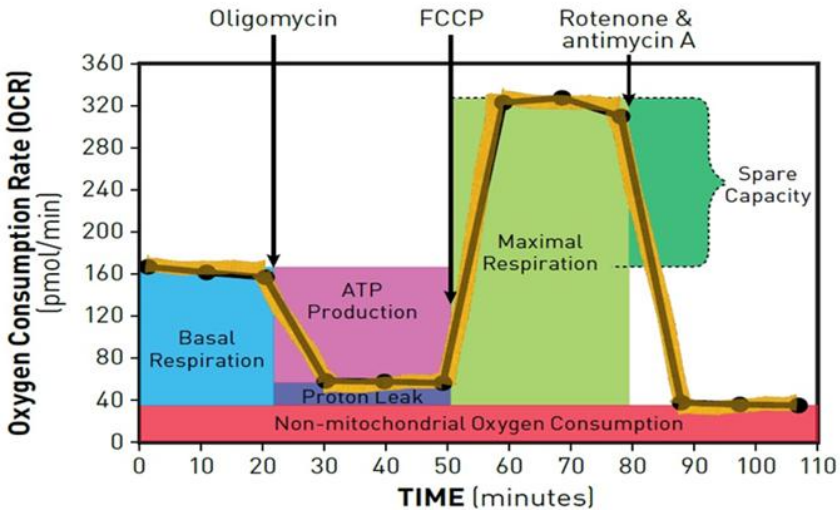

Figure 11. Example of Agilent Seahorse XF Cell Mito Stress Test profile, showing the key parameters of mitochondrial function determined by the assay

1) Basal respiration is measured before the injection of any compounds (blue).
2) The decline of OCR after oligomycin injection (pink) indicating the extent from ATP synthesis.
3) Maximal respiration is measured after FCCP injection, which uncouples mitochondrial respiration and thus allows the maximal oxygen consumption (light green).
4) Proton leak is calculated from the residual OCR after oligomycin injection (violet).
5) Non-mitochondrial respiration is measured after the addition of rotenone and antimycin A, representing oxygen consumption not linked to mitochondrial activity (red).
6) Spare respiratory capacity is the difference between maximal respiration and basal respiration, indicating the ability of a cell to respond to increased energy demands (green).

1.4.3. Flow cytometry

Flow cytometry and fluorescence-activated cell sorting (FACS), are technique used to analyse and sort cells based on their fluorescent characteristics, respectively. They are widely used in many fields, including immunology, cancer research, and cell biology. Flow cytometry provides exact and reliable data on the presence and the levels of diverse cellular components if they are fluorescent or can be rendered fluorescent using for example antibodies. As with any fluorescence method, correct experimental design with appropriate controls and careful sample preparation are essential in producing accurate and reliable data. If performed properly, flow cytometry provides valuable insights into cellular phenotypes and can significantly contribute to cancer research and diagnostics.

In this work, this technique was used to detect CAIX expression in human osteosarcoma 143B cells. For CAIX detection, an Alexa Fluor® 488-conjugated antibody against human CAIX (Catalog #: FAB2188G) was used; and a Mouse IgG2A Alexa Fluor® 488-conjugated antibody (Catalog #: IC003G) served as an isotype control.

Table 3. Advantages and drawbacks of flow cytometry.

Advantages	Drawbacks
High sensitivity and specificity for detecting protein expression.	Requires access to a flow cytometer and FACS-specific reagents
Ability to analyse large numbers of cells quickly	Possibility of non-specific binding demand extensive controls
Provides quantitative and qualitative data on protein expression	Cell preparation and antibody staining conditions must be optimized for each cell type
Can be combined with other markers for multi-parametric analysis	

1.4.4. Transfection

Transfection is a technique used in cellular and molecular biology to introduce nucleic acids (DNA or RNA) into eukaryotic cells to either create genetically altered cells or probe for the gene activity, protein expression. This method allows researchers to change gene abundance in cells, facilitating the investigation of biological pathways, processes, and reactions. There are three types of transfection. Chemical transfection uses chemical reagents to enable nucleic acids to be transported into cells. Common reagents are polymers, cationic lipids (lipofection), and calcium phosphate. Physical transfection involves physical methods such as electroporation, microinjection, or biolistic particle delivery to introduce nucleic acids into cells. Known sometimes as transduction, biological transfection uses viral vectors to introduce genetic material into cells.

In this work, polyethylenimine (PEI) transfection (Table 4) was chosen as the technique of CA9 gene deletion in human 143B cells. PEI transfection is one type of chemical transfection method whereby cationic polymer polyethylenimine introduces nucleic acids into cells. Particularly in mammalian cells, PEI is chosen for its remarkable transfection efficiency upon condensation of DNA into positively charged particles that can then interact with the negatively charged cell membrane. Reliable and repeatable results depend on thorough optimization of DNA-PEI condensation.

Table 4. Advantages and drawbacks of PEI transfection

Advantages	Drawbacks
High Efficiency	Can be cytotoxic at high concentrations
Compatible for many types of cells	Variations in PEI batches can compromise effectiveness
Cost-Effective	
Effective for both transient and stable transfections	

CRISPR/Cas9 system

CRISPR/Cas9 (Clustered Regularly Interspaced Short Palindromic Repeats/ CRISPR -associated protein 9) systems high specificity, efficiency, and simplicity of application have transformed genome editing. Originally identified as a component of a bacterial adaptive immune system, CRISPR

/Cas9 is now extensively applied in cancer biology to research gene function, validate medication targets, and generate treatment methods (Doudna & Charpentier, 2014).

Guided by synthetic single-guide RNA (sgRNA) complementary to the target sequence, CRISPR /Cas9 works by inducing a site-specific double-stranded break in DNA. The DSB is corrected by homology-directed repair, if there is a template supplied or by non-homologous end joining, resulting in frameshift mutations and gene knockout (Sander & Joung, 2014). Variations of the Cas9 enzyme, such the Cas9 nickase (D10A mutant) employed in this thesis, increase editing specificity by using two sgRNAs to cause a DSB, hence lowering off-target effects.

In this work, human osteosarcoma 143B cells were used to create CRISPR/Cas9 knockout of the *CA9* gene.

1.4.5. Western Blot

Western blotting, or immunoblotting, is a commonly employed laboratory technique used for the detection and analysis of specific proteins in biological samples, including tissue extracts and cell lysates. In this method proteins are firstly separated according to their molecular weight using SDS-PAGE, which denatures proteins and allows size-based separation. Following separation, proteins are transferred to a nitrocellulose or PVDF membrane, maintaining their spatial arrangement from the gel.

After transfer, the membrane is blocked to prevent non-specific binding sites and is subsequently incubated with a primary antibody that selectively binds the target protein. A secondary antibody, conjugated with an enzyme or fluorescent tag, attaches to the primary antibody, enabling the visualisation of protein bands through detection methods like chemiluminescence or colorimetric reactions. This assay confirms protein presence and offers semi-quantitative data on protein abundance, as well as information regarding molecular weight.

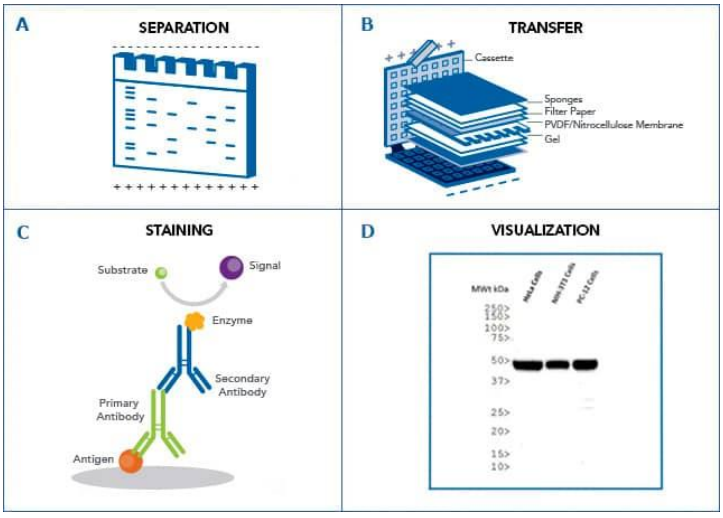

Figure 12. Steps of western blotting. (taken from novusbio.com)

Established in 1979, western blotting has emerged as a crucial method in molecular biology, biochemistry, and medical diagnostics. This method is widely employed to analyse protein expression, post-translational modifications. The technique's sensitivity and specificity, along with the availability of various antibodies, render it an essential tool in research and clinical laboratories.

1.4.6. Proteome Profiler Antibody Arrays

Proteome Profiler Antibody Arrays from R&D Systems are advanced multiplex assay tools for early-stage research. Allowing simultaneous measurement of more than 100 proteins within a single biological sample. This array provides a semiquantitative analysis of various protein targets, such as oncoproteins (array used in this work), cytokines, chemokines, phosphokinases, and other signalling molecules. This assay eliminates the requirement for specialised equipment or multiple Western blot experiments.

The assay uses nitrocellulose membranes that are spotted in duplicate with precisely chosen capture antibodies. Target proteins, from the sample, bind to their specific antibodies on the membrane. Detection is accomplished using biotinylated or HRP-conjugated secondary antibodies, followed by chemiluminescent visualisation, resulting in signals that correlate to the quantity of each protein present. This method enables researchers to efficiently analyse intricate protein signalling networks and changes in protein expression.

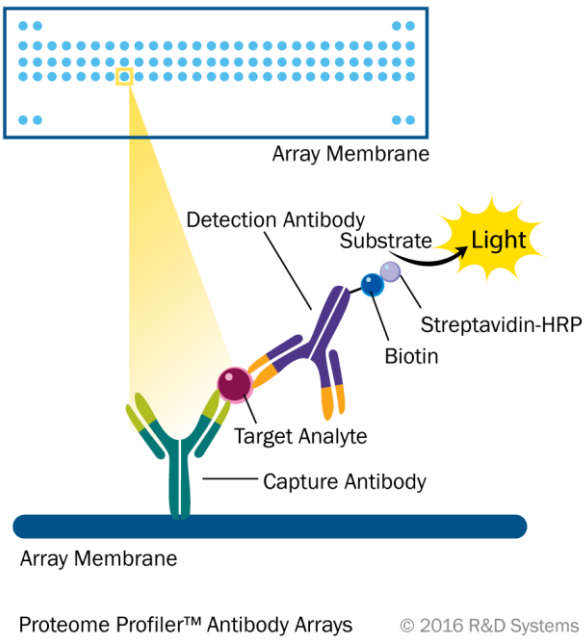

Figure 13. Antibody Array Principle. (taken from rndsystems.com)

2. Materials and Methods

2.1. Materials

2.1.1. Cell lines

143B is human osteosarcoma cell line (ATCC, CRL-8303).

2.1.2. CAIX inhibitors

VD11-4-2 3-(cyclooctylamino)-2,5,6-trifluoro-4-((2-hydroxyethyl)sulfonyl)benzenesulfonamide (later referred to as VD)

AZ19-3-2 N-[2-[2-(cyclooctylamino)-3,5,6-trifluoro-4-sulfamoyl-phenyl]sulfonylethyl]-3-[2-[2-[2-[2-[2-[2-[2-[2-[2-[2-[2-[3-[2-[2-(cyclooctylamino)-3,5,6-trifluoro-4-sulfamoyl-phenyl]sulfonylethylamino]-3-oxo-propoxy]ethoxy]ethoxy]ethoxy]ethoxy]ethoxy]ethoxy]ethoxy]ethoxy]ethoxy]ethoxy]ethoxy]ethoxy]propanamide (later referred to as AZ)

Structures of the inhibitors are shown in Figure 6.

2.1.3. Reagents

- 10 mM Tris HCl, pH 9.5
- Acetic acid
- Antibiotics solution (10000 units/ml penicillin and 10 mg/ml streptomycin) (Gibco)
- Bovine Serum Albumin (BSA), (Sigma)
- Dialyzed FBS (dFBS) (Gibco)
- Dimethyl sulfoxide (DMSO), (Carl Roth, ≥ 99, 5 %)
- Dulbecco's Modified Eagle Medium (DMEM) (Gibco)
- Ethylenediaminetetraacetic acid (EDTA)
- Fetal Bovine Serum (FBS) (Gibco)
- Glutamine, (Roth)
- Human Carbonic Anhydrase IX/CA9 Alexa Fluor 488-conjugated Antibody, (BioScience)
- Minimum Essential Medium Non-Essential Amino Acids (MEM NEAA), (Gibco)
- Mouse IgG2A Alexa Fluor 488-conjugated Antibody, (BioScience)
- Paraformaldehyde (PFA)
- Phosphate-buffered saline (PBS) pH 7,2 (1X) (Gibco)
- Riboflavin (RF)
- Sulforhodamine B (SRB), (Sigma)
- Trichloroacetic acid (TCA)

- Opti-MEM (Gibco)
- Proteome Profiler Human XL Oncology Array (R&D systems)
- RIPA lysis buffer (ThermoFisher)
- Halt Phosphatase Inhibitor Cocktail (ThermoFisher)
- Halt Protease Inhibitor Cocktail ThermoFisher)
- PMSF Protease Inhibitor (ThermoFisher)

2.1.4. Consumables and small equipment

- 10 cm Cell culture dishes, (Techno Plastic Products (TPP))
- 6-well, 12-well, 24-well and 96-well plates, (TPP)
- Centrifuge tubes 15 ml, 50 ml (Thermo Scientific)
- Electroporation cuvettes
- Microcentrifuge tubes 1.5 ml, 2 ml (Thermo Scientific)
- Multichannel pipettes 300 µl (Eppendorf)
- Pipette tips 10 µl, 200 µl, 1000 µl (Eppendorf)
- Serological pipettes 1 ml, 5 ml, 10 ml, 25 ml (Thermo Scientific)
- Single channel pipettes 10 µl, 200 µl, 1000 µl (Eppendorf)
- T75 and T182 flasks (TPP)

2.1.5. Equipment

- Electroporator
- Flow cytometer
- CO_2 incubator (Binder)
- Laminar flow cabinet
- Centrifuge
- Microcentrifuge (Eppendorf)
- Seahorse XF Pro Analyzer (Agilent)
- Alliance Q9 Advanced (UVITEC)

2.1.6. Software

- Excel 2016 (Microsoft)
- MatLab
- FCS Express 5 (De Novo Software)
- Seahorse Wave Desktop Software 2.6.1 (Agilent)
- Flowing Software 2.5.1 (Turku Bioscience)

2.2. Methods

2.2.1. Cell culture

143B human cancer cells were grown in high glucose (4.5 g/l) DMEM medium supplemented with 10% FBS, 10000 units/ml of penicillin and 10µg/ml of streptomycin (later referred to as medium). Cells cultured in humidified CO_2 incubator at 37°C and 5% CO_2. Cells were split after reaching 70% confluence.

For metabolic reprograming experiments cells were cultured in O-DMEM supplemented with either 10% or 1% dFBS, 4 mM glutamine and when indicated 1 µM RF (later referred to as deficient medium).

2.2.2. Cell thawing

Cryovials with frozen cells were thawed in 37°C water bath for ~2 min. Freshly thawed cell suspension was transferred to 10 ml of pre-warmed medium and centrifuged for 3 min at 350 RCF. The supernatant was removed, cells resuspended in 15 ml of medium and transferred to T75 flask. After 24h medium was discarded and fresh growth medium added to the cells. Cells were cultivated until they reached 70% confluence.

2.2.3. Cell subculturing

The old medium was discarded; cells were washed with 2 ml of PBS. PBS was discarded and 2 ml of 0.5 mM EDTA was added. Cells were incubated at 37 °C for 5-10 min, until detached. Then 8 ml of culture medium was added, cells were resuspended and plated to a new cell culture flask. Cells cultured in humidified CO_2 incubator at 37°C and 5% CO_2 until they reach 70% confluence.

2.2.4. Cell Freezing

The old medium was discarded; cells were washed with 2 ml of PBS. PBS is discarded and 2 ml of 0.5 mM EDTA transferred. Cells were incubated at 37 °C for 5-10 min, until detached. Then 8 ml of culture medium was added, cells were resuspended and transferred to 50 ml centrifuge tube. Cells were centrifuged at 350x RCF, for 3 min., supernatant was discarded and cells were resuspended in 4 ml cold growth medium supplemented with 10% DMSO. Then cell suspension was aliquoted to cryotubes. Cryotubes were stored at -4°C for 2h, then transferred to -80°C for 2-4 days. Finally, frozen cells were transferred to a liquid nitrogen dewar for the long-term storage.

2.2.5. Plasmid amplification and purification

Plasmid used to create CAIX-knockout cells

In this work the CA IX Double Nickase Plasmid (h) (Catalogue #: sc-400905-NIC, Santa Cruz) (Figure 14) was used to target the CA9 gene, which is found at the cytogenetic locus 9p13.3 on the

short arm of chromosome 9 in humans, to create CAIX-knock out 143B cell line. Using a highly precise CRISPR/Cas9 double nicking strategy, which generates two neighbouring single-stranded breaks simulating a double-stranded break. This plasmid system is intended to inhibit CA9 gene expression. Two plasmids make up the system: each one codes a D10A-mutated Cas9 nickase and a unique 20-nucleotide guide RNA (gRNA) that hooks to a particular target sequence in the CA9 gene. The gRNA sequences A: 5'-cccggagaggatctacc-3', and B: 5'-tctgggtgaatccttcac-3'. About 20 base pairs offset these gRNAs to improve selectivity and lower off-target cleavage. One plasmid carries a GFP reporter to provide visual confirmation of transfection; the other has a puromycin resistance gene, allowing selection of effectively transfected cells.

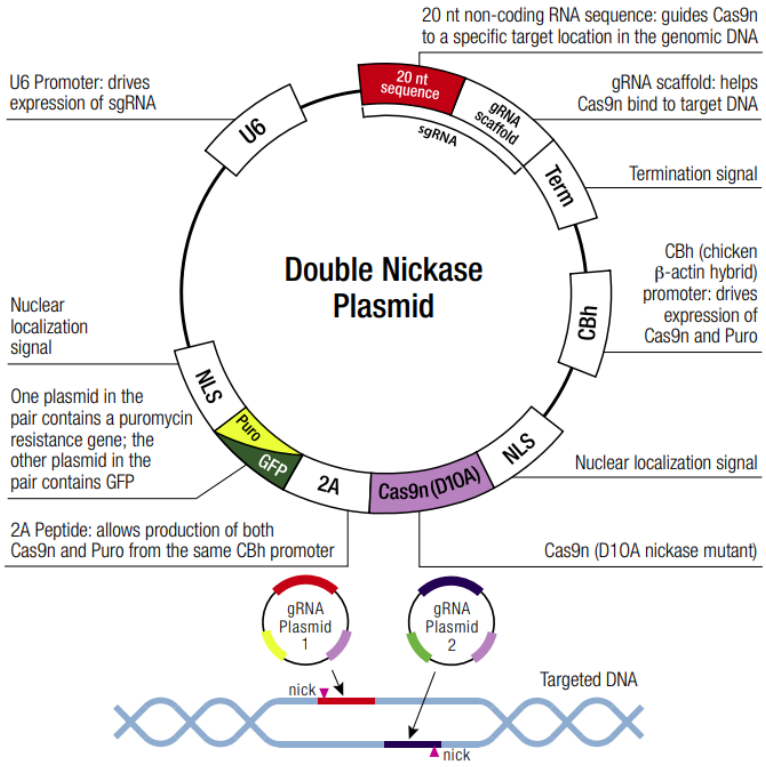

Figure 14. CA IX Double Nickase Plasmid (h) construct.

Bacterial transformation and plasmid amplification

A couple of the CAIX-specific Double Nickase plasmids (two vectors with different CAIX-targeting sequences and different eukaryotic selection markers) were amplified by using chemically competent-*E. coli* cells (DH5α strain). A mixture containing 30 µl of DH5α cells and 1 µl of 0.1 mg/ml plasmid was prepared. The mixture was then incubated on ice for 10 min. Afterwards, the cells underwent heat shock at 42°C for 42 sec. followed by an additional 5 minute incubation on ice. Finally, transformed bacteria cells were plated on LB agar plate supplemented with ampicillin. Bacteria was cultivated overnight at 37°C. Next day, a bacterial colony from the plate was transferred to a flask containing 150 ml of LB medium with 100 µg/mL ampicillin. Cells were incubated overnight at 37°C with vigorous shaking (approx. 230 rpm).

Plasmid purification

The plasmids were purified using QIAGEN Plasmid Maxi Kit. The overnight culture of bacterial cells was harvested by centrifugation at 6000 × g for 15 min at 4°C. The resulting pellet was carefully resuspended in 10 mL of Buffer P1 by pipetting up and down until no cell clumps remained. To this suspension, 10 mL of Buffer P2 was added and mixed thoroughly by inverting the tube 4−6 times, followed by incubation at RT for 5 min. Afterwards, 10 mL of pre-chilled Buffer P3 was added, mixed immediately by inverting the tube 4–6 times, and then incubated on ice for 20 min. Lysate was centrifuged at 20000 × g for 10 min at 4°C and the resulting supernatant, containing the plasmid DNA, was carefully removed.

Next step was to equilibrate the QIAGEN-tip with 10 ml of Buffer QBT by allowing it to pass by gravity flow. The supernatant, containing DNA, was then added to the equilibrated QIAGEN-tip, allowing it to enter the resin via gravity flow. Afterwards, the QIAGEN-tip was washed twice with 30 ml of Buffer QC, again draining it by gravity flow. Plasmid DNA was eluted with 15 mL of Buffer QF into a 50 ml falcon tube.

0.7 volumes (10.5 ml) of isopropanol was added to the eluate in order to precipitate DNA. The mixture was centrifuged at 15,000 x g for 30 min at 4°C. The supernatant was carefully removed and DNA pellet was washed with 5 ml of 70% ethanol, then centrifuged at 15,000 x g for 10 min. The supernatant was carefully discarded and DNA pellet was air-dried for 5–10 min. Finally, the DNA was dissolved in 500 µl of EB buffer. Plasmid solution was transferred to -20°C for long-term storage.

2.2.6. PEI transfection

143B cells were seeded in 6-well plate at 1.5×10^5 cells per well. Cells cultured in humidified CO_2 incubator at 37°C and 5% CO_2 for approximately 20 h. The old medium was gently aspirated and 3 ml of fresh medium was added. The next step was to prepare the DNA:PEI mixture at a ratio of 1:6. Firstly, 6 µg of DNA was diluted into 50 µL of Opti-MEM. Then, 18 µl of PEI (1 mg/ml) was diluted into 50 µl of Opti-MEM. The diluted PEI was gently added to the diluted DNA. The mixture was incubated for about 10 min at RT. After incubation, 100 the µL transfection mix was carefully added dropwise to each well with 143B cells. The cells were incubated overnight in humidified CO2 incubator at 37°C and 5% CO_2. The following day, the medium was carefully aspirated and replaced with 3 ml of fresh medium in each well. Transfection efficiency was assessed by the amount of green fluorescent protein expression using flow cytometry.

Transfected cells were first selected based on green fluorescent protein expression by sorting cells. Then, additional selection was performed by growing the cells in medium containing various concentrations of puromycin (0, 0.5, 1, 1.5 µg/mL) in 10 cm culture plates. Survived 143B cell colo-

nies were picked, transferred to 24-well plates with medium and subcultured over several weeks moving from 12-well plates to, finally, 10 cm cell culture plates. Afterwards, clones were frozen and stored in liquid nitrogen dewar.

2.2.7. Western Blot

To confirm that the *CA9* gene knockout was successful Western Blot analysis was performed.

143B WT and KO cells were seeded in a 10 cm plate at 2.5×10^5 cells per plate in medium. Cells cultured in humidified CO2 incubator at 37°C and 5% CO_2 in either normoxic (21% O_2) or hypoxic (1% O_2) conditions for approximately 72 h. After three days, 143B cells were harvested, washed with PBS twice, and resuspended in RIPA lysis buffer containing protease and phosphatase inhibitors for 30 min on ice. The the cells were centrifuged at 16000× g for 15 min at 4°C. Supernatant collected and total protein lysate was quantified by the Bradford method. Lysates were boiled for 10 min at 95°C in 6X LDS sample buffer containing β-ME. Samples loaded 50 µg per sample, equal volumes, separated using polyacrylamide gel, and transferred onto 0.2 µm nitrocellulose membrane. then, the membrane was blocked using 2% milk-TBST (1X Tris-Buffered Saline, 0.1% Tween 20 detergent) for 1 hour and incubated overnight at 4°C with primary antibodies anti-hCAIX M75 in 2% milk-TBST. β-actin was used as the protein loading control. Membrane was then washed three times for 5 min in TBST and incubated for 1 hours at room temperature with a secondary anti-mouse antibody, washed an additional three times, and then incubated using Novex ECL Chemiluminescent Substrate Reagent Kit substrate. Bands were visualized using Alliance Q9 Advanced.

2.2.8. AlamarBlue and SRB assays

Preparation of cells for AlamarBlue and SRB assays

143B WT and KO cells were seeded in a 96-well plate at 1.5×10^3 cells per well in deficient medium with 10% of dFBS, ±RF for AlamarBlue assay. For SRB assay, 143B WT cells were seeded at 1.5×10^3 cells per well in a 96-well plate in medium with glucose or galactose. For both assays cells were cultured in humidified CO_2 incubator at 37°C and 5% CO_2 for approximately 48 h. After two days, CAIX inhibitors (VD11-4-2 and AZ-19-3-2) were added to the cells at different concentrations (0, 2.10, 2.62, 3.28, 4.10, 5.12, 6.4, 8 µM). After three days, AlamarBlue or SRB assay was performed.

AlamarBlue assay

Cells were incubated with 10% AlamarBlue for 2 hours under normoxic conditions at 37°C. The fluorescence signal was quantified with a multi-mode microplate reader at 580 nm, using an excitation wavelength of 540 nm. The response to treatments was quantified by assessing LC_{50} values, defined as the concentration of inhibitor that results in a half-maximum viability response, as determined by Hill fitting.

SRB assay

First, the 96-well plate was tapped upside down to remove the old deficient medium, repeating this process multiple times on a napkin to ensure all wells were as dry as possible. Then, 200 µL of PBS per well were added, and the PBS was removed by tapping the plate upside down. Next, 100 µL of cold 10% TCA were added to fix the attached cells. The plate was incubated at +4°C for 1 hour. After incubation, the plate was tapped again to remove the TCA. The cells were then washed with 200 µL of dH_2O to remove any leftover TCA. Afterwards, the plate was dried with an air dryer. Subsequently, 100 µL of 0.04% SRB in 1% acetic acid were added and the plate was incubated for 30 min at RT in the dark. The SRB reagent was removed by tapping, and the excess dye was washed off with 100 µL of 1% acetic acid, which was then removed by tapping. Lastly, the cells were resuspended in 100 µL of 10 mM Tris (pH 9.5) and the samples were transferred into a new 96-well plate. Absorption was measured at 560 nm. The response to treatments was quantified by assessing LC_{50} values, defined as the concentration of inhibitor that results in a half-maximum viability response, as determined by Hill fitting.

2.2.9. Flow cytometry

Cell Culture for flow cytometry

143B cells were seeded in a 6-well plate at 2×10^4 cells per well in deficient medium with 10% dFBS, ±RF. Cells cultured in humidified CO_2 incubator at 37°C and 5% CO_2 for approximately 48 hours. After two days, CAIX inhibitors VD11-4-2 and AZ-19-3-2 were added to the cells at concentrations ranging from 0 µM to 5 µM. After three days, CAIX immunofluorescent staining and flow cytometry was performed.

Anti-CAIX antibody staining and measurement

The old deficient medium was discarded, and the cells were washed with 1 ml of PBS. Then, 200 µL of 0.5 mM EDTA was added to each well and incubated for 5-10 min, until the cells were completely detached. The cells were then resuspended in 800 µL of deficient medium, transferred to a microcentrifuge tube, and centrifuged at 300×g for 3 min at +4°C.

All subsequent steps were performed on ice. The supernatant was discarded, and the cells were resuspended in 200 µL of FACS buffer (PBS + 0.5% BSA + 2.5 mM EDTA). The cell suspension was divided into two new microcentrifuge tubes and centrifuged again at 300×g for 3 min at +4°C. The supernatant was removed and 100 µL of diluted antibody was added and mixed with the cells. The mixtures were incubated for 30 min on ice, then centrifuged again at 300×g for 3 min at +4°C. The supernatant was discarded, and the stained cells were washed with 500 µL of FACS buffer three times. Finally, the cells were resuspended in 600 µL of FACS buffer and fixed with 200 µL of 4% PFA

(resulting in a final concentration of 1% PFA). Flow cytometry analysis was performed within 24 hours after fixing the cells.

2.2.10. Seahorse assay

Cell culture for the Seahorse assay

143B cells were seeded at 1×10^3 cells per well in a 96-well Seahorse XF cell culture plates in deficient medium with 10% dFBS, ±RF. Cells cultured in humidified CO_2 incubator at 37°C and 5% CO_2 for approximately 48 hours. After two days, CAIX inhibitors VD11-4-2 and AZ-19-3-2 were added to the cells at concentrations ranging from 0 µM to 5 µM. After three days, the Seahorse assay was performed.

Seahorse assay

The day before the assay, the sensor cartridge was hydrated with 200 µL of Seahorse XF Calibrant buffer and incubated at 37°C without CO_2 overnight. Additionally, assay medium was prepared by adding 2 g/L of glucose and 4 mM of glutamine to O-DMEM.

On the day of the assay, the old deficient medium was discarded from the cells. The cells were washed once with 175 µL of Seahorse assay medium. After washing, 175 µL of Seahorse assay medium was added to each well, and the plate was placed in a 37°C incubator without CO_2 for an hour.

During the incubation, solutions of the inhibitors to be used for the assay were prepared, using assay medium, at following concentrations: oligomycin 8 µM, FCCP 18 µM, antimycin A and rotenone 6 µM. Then, 25 µL of each inhibitor was loaded into the corresponding ports of the cartridge.

After the incubation, the Seahorse assay was performed. After the measurement, the assay medium was discarded, the dry the plate was stored at -80°C until protein concentrations could be measured with the Micro BCA Protein Assay Kit. Protein concentrations were used to normalize the Seahorse data as described below.

Normalization of Seahorse measurement

Cell lysis

The plate with cells was removed from -80°C, and 75 µL of dH_2O was added to each well. Cells were lysed thoroughly by scraping and pipetting them up and down. Subsequently, 50 µL of the lysate from each cell was transferred to a new 96-well plate, and 100 µL of dH_2O was added to each well.

Normalization procedure

After lysing the cells, BSA standard was diluted in dH_2O as detailed in Table 3. Additionally, Micro BCA Working Reagent (WR) was prepared by mixing 25 parts of Micro BCA Reagent MA, 24 parts of Reagent MB, and 1 part of Reagent MC (25:24:1, MA:MB).

Table 5. Preparation of diluted BSA standard

Vial	Volume of dH_2O	Volume and Source of BSA	Final BSA Concentration
1	1350 µL	150 µL of BCA stock	200µg/mL
2	800 µL	800 µL of previous dilution	100µg/mL
3	720 µL	480 µL of previous dilution	40µg/mL
4	600 µL	600 µL of previous dilution	20µg/mL
5	600 µL	600 µL of previous dilution	10µg/mL
6	600 µL	600 µL of previous dilution	5µg/mL
7	600 µL	600 µL of previous dilution	2.5µg/mL

Once prepared, 150 µL of each standard was pipetted into the 96-well plate with the diluted samples. Then, 150 µL of WR was added to each well and the plate was thoroughly mixed on a plate shaker for 30 seconds. The plate was covered using the Sealing Tape for 96-Well Plates and incubated at 37°C for 2 hours. After incubation, the plate was cooled to RT and the absorbance was measured at 560 nm.

2.2.11. Proteome Profile assay

Procedure was done using Proteome Profiler Human XL Oncology Array kit, by manufacturer's protocol.

Briefly, 143B cell lysates were prepared using RIPA lysis buffer supplemented with protease and phosphatase inhibitors (Halt Phosphatase Inhibitor Cocktail, Halt Protease Inhibitor Cocktail, and PMSF Protease Inhibitor). The preparation occurred over 30 minutes on ice, followed by centrifugation at 16,000 × g for 15 minutes at 4°C. The Bradford method was employed to quantify total protein lysate. 20 µg of lysate were utilised for each condition. Images were acquired utilising the Alliance Q9 Advanced (UVITEC) system. Spots were quantified utilising the UVIBAND MAX analysis software system. The pixel density signal for each spot, indicative of a single analyte, was quantified. Each analyte was measured in duplicate, and the average of each pair was calculated. The quantified average signal value for each spot was adjusted by subtracting the average background value, which served as the negative control in the array kit.

List of proteins, which expression is compared.

1. Growth Factors and Receptors
   1.1. EGF R/ErbB1: epidermal growth factor receptor, a receptor tyrosine kinase involved in cell proliferation, differentiation, and survival.
   1.2. FGF basic: basic fibroblast growth factor, part of the FGF family, which regulates cell growth, development, and tissue repair.

1.3. Endoglin/CD105: a co-receptor for TGF-beta, highly expressed in proliferating endothelial cells and involved in angiogenesis and vascular development.

1.4. Axl: a receptor tyrosine kinase of the TAM family, mediates cell survival, proliferation, migration, and immune regulation.

2. Enzymes

2.1. ENPP-2/Autotaxin: an ectoenzyme that generates lysophosphatidic acid, stimulating cell motility, proliferation, and wound healing.

2.2. u-Plasminogen Activator/Urokinase: a serine protease involved in the degradation of the extracellular matrix and tissue remodelling.

3. Transcription Factors

3.1. HNF-3β (FOXA2): a member of the hepatocyte nuclear factor family, crucial for embryogenesis and differentiation of the gastrointestinal tract.

3.2. HO-1/HMOX1: heme oxygenase 1, an inducible enzyme with antioxidant and cytoprotective functions, regulated at the transcriptional level.

3.3. p53: a tumour suppressor transcription factor that regulates the cell cycle and apoptosis.

4. Adhesion Molecules and ECM Proteins

4.1. Osteopontin: a glycoprotein involved in cell adhesion, migration, and signalling.

4.2. Tenascin C: an extracellular matrix protein involved in tissue remodelling and cell adhesion.

4.3. Vimentin: an intermediate filament protein, marker of mesenchymal cells, involved in maintaining cell integrity and migration.

5. Cell Death and Survival Regulators

5.1. Survivin: an inhibitor of apoptosis protein (IAP) family member, regulates cell division and inhibits apoptosis.

5.2. Serpin E1/PAI-1: plasminogen activator inhibitor-1, regulates fibrinolysis and cell migration.

6. Lectins and Glycan-Binding Proteins

Galectin-3: a beta-galactoside-binding lectin involved in cell-cell and cell-matrix interactions, apoptosis, and immune responses.

3. Results

3.1. Establishment of the experimental system

Previous experiments in the lab showed, that the CAIX inhibitors VD and AZ were not as effective *in vivo* as the *in vitro* tests had indicated. Therefore, the main goal of this project was testing the possibility that metabolic reprograming of cancer cells, sensitize them to CAIX inhibitors, subsequently resulting in synthetic lethality.

3.1.1. Determination of the optimal experimental setup by flow cytometry

To achieve the set goal, it was crucial first to determine the conditions in which CAIX was expressed in live 143B cancer cells. Several different cell cultivation conditions were tested, all comparing cells grown with and without RF. Also, cells were grown with different dFBS concentrations: 10%, 5%, and 1%. After 5 days of incubation in humidified CO_2 incubator at 37°C and 5% CO_2, cells from different experimental conditions were collected, stained with CAIX antibodies, and analysed by flow cytometry. This process allowed to identify the optimal conditions for CAIX expression. By analysing the data, we could determine the specific conditions under which CAIX expression was maximized, providing a solid foundation for subsequent experiments focused on metabolic reprogramming and inhibitor sensitivity.

Table 6. CAIX expression in 143B cells obtained by flow cytometry.

dFBS concentration, %	**CAIX expression in 143B cells, % of total cell population**	
	With RF	Without RF
10	10.4	21.1
5	12.5	21.4
1	22.8	41,0

From the results, we can see that cells grown with 10% and 5% dFBS did not show significant differences in CAIX expression in 143B cells (Figure 15 and Table 6). Moreover, CAIX was expressed only when cells were grown without RF, with the percentage of the total cell population expressing CAIX being around 21%, while in cells with RF, the percentage was around 10-12%. Taking this into consideration, a medium with 10% dFBS was chosen for further experiments, as it provides less stressful conditions for the cells and better supports their growth and viability.

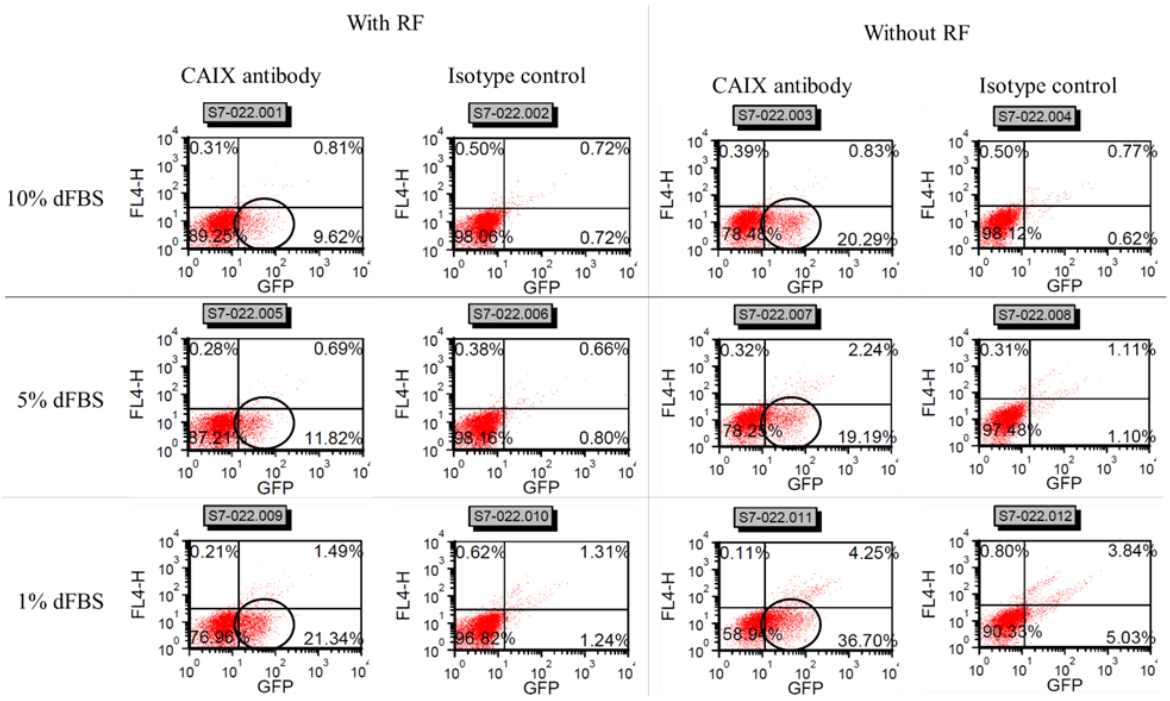

Figure 15. CAIX expression in 143B cells grown in different experimental conditions. CAIX positive cells circled.

An interesting result was observed with cells grown with only 1% dFBS. These cells showed the ability to express CAIX when grown both with and without RF; however, under the latter condition, cells were highly stressed and grew much slower. The percentage of the total cell population expressing CAIX in cells grown with RF was around 23%, and without RF was around 41%. This suggests that while low dFBS conditions can enhance CAIX expression, the associated stress negatively impacts cell growth. Thus, a trade-off between the CAIX expression and cell health and proliferation turned out to be a key consideration for optimizing experimental conditions.

3.1.2. Inactivation of mitochondrial respiration

To verify the inhibitory effect of RF deficiency on the mitochondria of live cells under the selected conditions, a Seahorse assay was performed. In this assay, cell mitochondrial respiration is measured by following the oxygen consumption rate (OCR). Agilent Seahorse XF Analyzer perform automatic, real-time measurements of OCR in live cells in a multi-well plate, examining key cellular functions like mitochondrial respiration and glycolysis. The analyser allows addition of compounds in a predetermined time sequence which enables in-depth analyses of different aspects of mitochondrial function. Using the Seahorse assay, we hoped to see how the RF deficiency affects tumour cell bioenergetics and to gain insights into mitochondrial activity and metabolic adaptability under different experimental conditions.

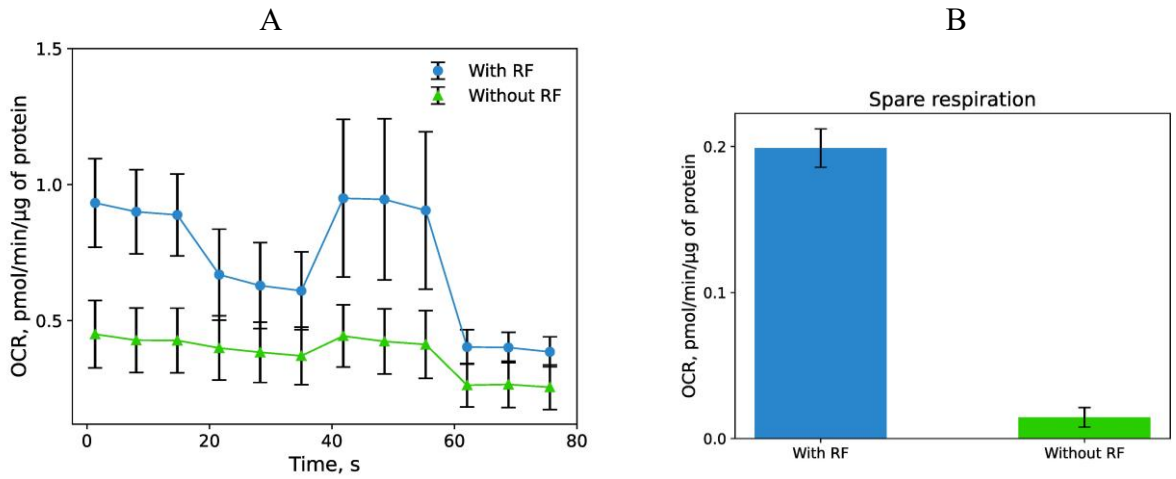

Figure 16. RF deficiency suppresses the respiration of 147B cells. A – OCR; B – spare respiratory capacity.

By analysing the respiration data, especially the basal respiration and maximum respiration points, it is evident that cultivating the cells without RF indeed significantly suppresses mitochondrial respiration (Figure 16), as there is a clear difference in the OCR values when comparing the two cell cultivation conditions (with and without RF). In addition, a very strong shift in spare respiratory capacity can be observed: with RF, the value is 0.17 OCR, and without RF, it is 0.01 OCR. This significant reduction in spare respiratory capacity suggests that RF deficiency severely impairs the cells' ability to respond to metabolic stress, indicating a compromised mitochondrial function. Such insights are valuable for understanding the metabolic impact of RF deficiency and can help making strategies to target mitochondrial pathways more effectively in future experiments. Additionally, the observed differences in OCR values emphasize the importance of considering metabolic status when evaluating cellular responses to various treatments.

3.1.3. Determination of effective and toxic concentrations of inhibitors in cancer cells

The last step in setting up the experimental conditions was to determine the effective and toxic concentrations of CAIX inhibitors in 143B cancer cells. This step is crucial for ensuring that the inhibitors are used in a relevant range that is at concentrations that maximize their efficacy while minimizing potential side effects.

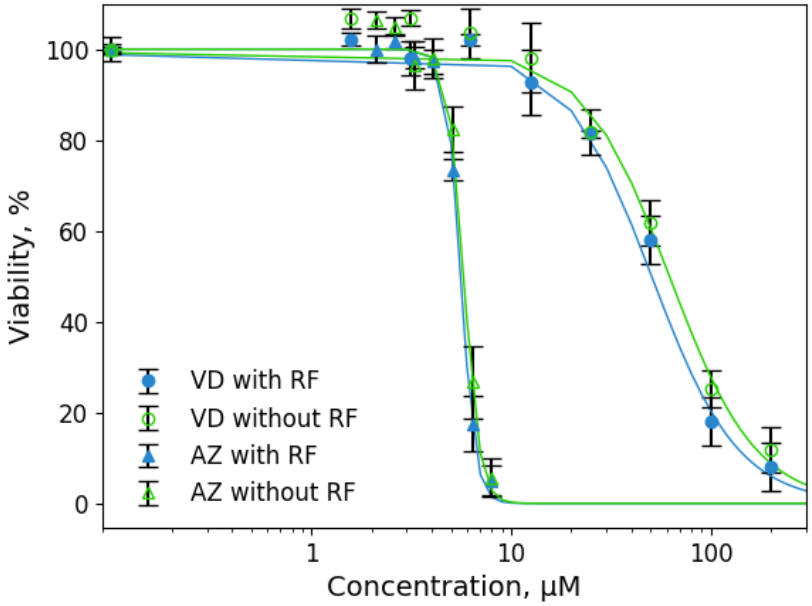

Figure 17. CAIX inhibitor effect on 143B cells viability ±RF (n=3).

Table 7. CAIX inhibitor LC_{50} values in 143B cells

CAIX inhibitor	**LC_{50} in live 143B cells, µM**	
	With RF	Without RF
VD	50.5	62
AZ	5.6	5.8

Between the two cell cultivation conditions, with and without RF, no significant differences could be seen at lethal inhibitor concentrations. It noteworthy that the lethal inhibitor concentrations were rather high, above 1 µM (Figure 18 and Table 9). Experimentally determined LC_{50} values were higher for VD with RF, VD 50.5 µM, AZ 5.6 µM; and without RF, VD 62 µM, AZ 5.8 µM. The high LC_{50} values suggest that the inhibitors may be binding unspecifically, which could have implications for their potential clinical use. This information is crucial for optimizing dosing regimens and assessing the feasibility of these inhibitors in therapeutic settings. Additionally, the lack of significant differences between conditions underscores the need for further investigation into alternative strategies or combinations of inhibitors to enhance efficacy.

3.2. Analysis of CAIX inhibitor effects on cancer cells

Since the toxicity determined with the AlamarBlue assay did not seem to depend sufficiently on CAIX expression under used experimental conditions, so an assay was employed focusing on the CAIX-positive cells.

3.2.1. Flow cytometry measurement of CAIX expression after inhibitor treatment

Using flow cytometry, it was possible to titrate inhibitor concentrations from 50 µM for VD and 5 µM for AZ down to 1 µM and 0.5 µM, respectively. The data indicated that concentrations lower than 4 µM for VD did not exhibit CAIX expression changes in 143B cells. For AZ, effects on CAIX expression was apparent at 2 µM, with no noticeable differences at lower concentrations (Figure 18 and Tables 10, 11). These findings highlight the sensitivity of the flow cytometry approach in detecting CAIX-dependent effects and underscore the importance of optimizing inhibitor concentrations to accurately assess their impact on CAIX expression and related toxicities. The ability to precisely determine effective concentrations aids in fine-tuning experimental conditions and improving the overall efficacy and safety profiles of CAIX inhibitors.

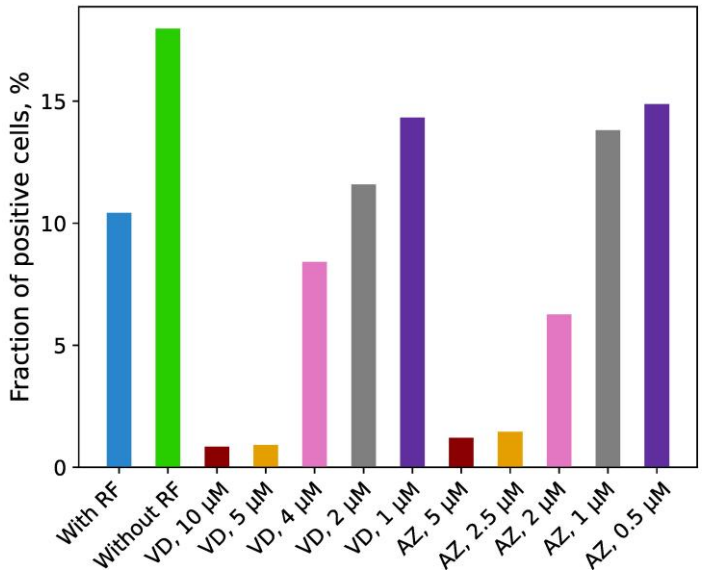

Figure 18. VD's and AZ's inhibitory effects on CAIX expression in 143B cells.

Table 8. VD's inhibitory effects on CAIX expression in 143B cells.

Inhibitor concentration, µM	CAIX expression in 143B cells, % of total cell population
10	1.1
5	1.7
4	9.5
2	12.7
1	14.3

Table 9. AZ‘s inhibitory effects on CAIX expression in 143B cells

Inhibitor concentration, µM	CAIX expression in 143B cells, % of total cell population
5	1.7
2.5	2.0
2	7.2
1	14.8
0.5	16.0

3.2.2. Seahorse assay to see inhibitors effect

To evaluate the toxicity of CAIX inhibitors on the respiration of live cells under the specified conditions (10% dFBS, ±RF), a Seahorse assay was conducted. This method, as previously mentioned, allows for the observation of changes in mitochondrial OCR over time. The results indicated that effective inhibitor concentrations can be as low as 1.5 µM for AZ and 4 µM for VD (Figure 20). These concentrations are at least five times lower than those determined by the SRB assay, suggesting they are more appropriate for assessing toxicity. Additionally, the Seahorse assay provides a more nuanced understanding of how these inhibitors impact mitochondrial function, offering insights that are critical for optimizing therapeutic strategies and improving the accuracy of toxicity evaluations.

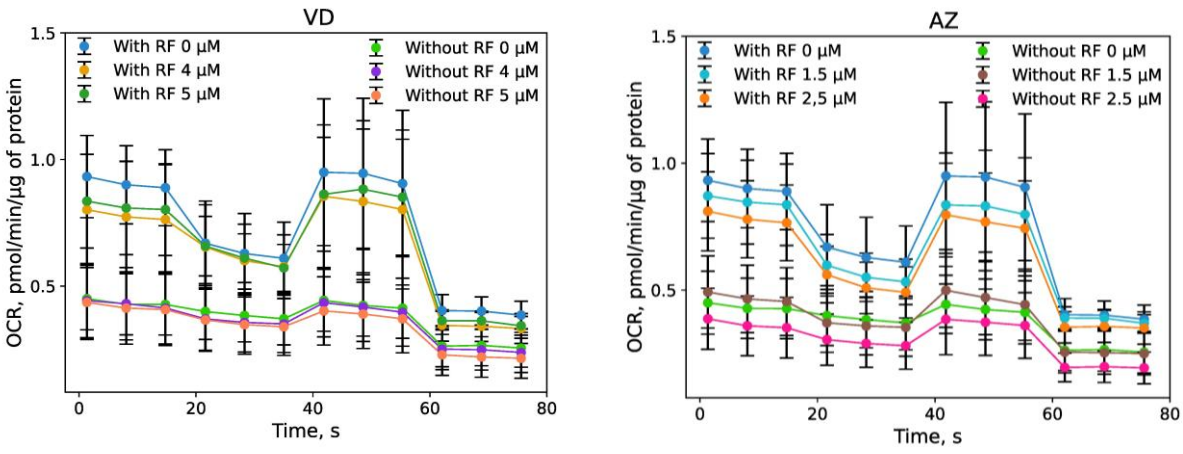

Figure 19. Seahorse assay results; CAIX inhibitors effects on mitochondrial respiration (n=3).

3.3. Protein Profiler assay

To determine changes in expression of oncoproteins in 143B cells grown in different condition, Proteome Profiler Human XL Oncology Array kit was used. Protein biomarkers of three experimental conditions (+RF 0 µM AZ, +RF 0 µM AZ and –RF 1 µM AZ) are compared (Figure 21). Every column in the table shows a distinct comparison. The values show the relative expression of protein. The

colour scheme emphasises whether in the first condition relative to the second, protein is expression higher (blue) or lower (red).

3.3.1. Comparison of +RF 0 µM AZ against +RF 1 µM AZ

Different expression of several proteins was seen in the comparison of 143B cells maintained under normal riboflavin conditions without CAIX inhibitor (+RF 0 µM AZ) to those treated with the CAIX inhibitor +RF 1 µM AZ. As blue colouring and expression ratios above one emphasise, Endoglin/CD105, Axl, HNF-3β, Galectin-3, and Serpin E1/PAI-1 all demonstrated greater expression under normal conditions. Endoglin/CD105 and Axl are important in angiogenesis and cell survival, their higher levels in normal settings imply that CAIX inhibition reduces processes promoting vascular growth and cell survival signalling. Indicating that these regulatory and adhesion-related pathways are downregulated when CAIX is inhibited. HNF-3β, a transcription factor essential for differentiation, and Galectin-3, which affects cell adhesion and immunological responses, were likewise less expressed when CAIX was inhibited. Serpin E1/PAI-1, a fundamental regulator of fibrinolysis and cell migration, higher expression in normal conditions, indicates that CAIX suppression greatly reduces anti-fibrinolytic and migratory signalling.

	+RF 0 µM AZ/+RF 1 µM AZ
HO-1/HMOX1	0.20
Vimentin	0.35
Survivin	0.72
FGF basic	0.80
EGF R/ErbB1	0.83
Osteopontin	0.84
ENPP-2/Autotaxin	1.66
Endoglin/CD105	2.00
Tenascin C	2.78
p53	2.83
Axl	4.49
HNF-3β	5.05
u-Plasminogen Activaror/Urokinase	5.92
Galectin-3	6.27
Serpin E1/PAI-1	32.40

Figure 20. Protein biomarkers comparison between +RF 0 µM AZ/+RF 1 µM AZ.

Expression ratios below one suggest that Vimentin, FGF basic, and Osteopontin all are expressed less in normal conditions. These proteins, linked to mesenchymal phenotype (Vimentin), growth factor signalling (FGF basic), and cell adhesion and migration (Osteopontin), seem to be upregulated by CAIX inhibition. Their higher expression upon CAIX inhibition might suggest an adaptive cellular response meant to preserve migratory and proliferative capacity under metabolic stress.

These data all together show that CAIX inhibition in the presence of riboflavin modulates the proteomic landscape of osteosarcoma cells: it downregulates those engaged in angiogenesis, differentiation, cell adhesion, and anti-fibrinolytic activity while upregulates proteins linked to migration

and growth factor signalling. This pattern implies that CAIX inhibition may both decrease important survival and migratory pathways, therefore sensitising cells to additional therapeutic intervention, and increase some elements of cellular adaption to stress.

3.3.2. Comparison of -RF 1 µM AZ against +RF 1 µM AZ

Different patterns can be seen, when comparing normal riboflavin concentration with CAIX inhibitor (+RF 1 µM AZ) vs riboflavin depletion with CAIX inhibitor (-RF 1 µM AZ) (Figure 21). Elevated expression in the -RF 1 µM AZ condition (values over 1, blue) of proteins including Serpin E1/PAI-1, HO-1/HMOX1, Galectin-3, p53, HNF-3β, Axl, Endoglin/CD105, and survivin. With increasing expression of proteins involved in anti-apoptosis (Survivin, Serpin E1/PAI-1), antioxidant defence (HO-1/HMOX1), cell adhesion and migration (Galectin-3, Axl, Endoglin/CD105), and cell cycle regulation (p53, HNF-3β), riboflavin depletion in the presence of CAIX inhibition triggers a strong stress-adaptive response. These modifications imply that by activating survival and repair processes, the cells try to offset metabolic and environmental stress.

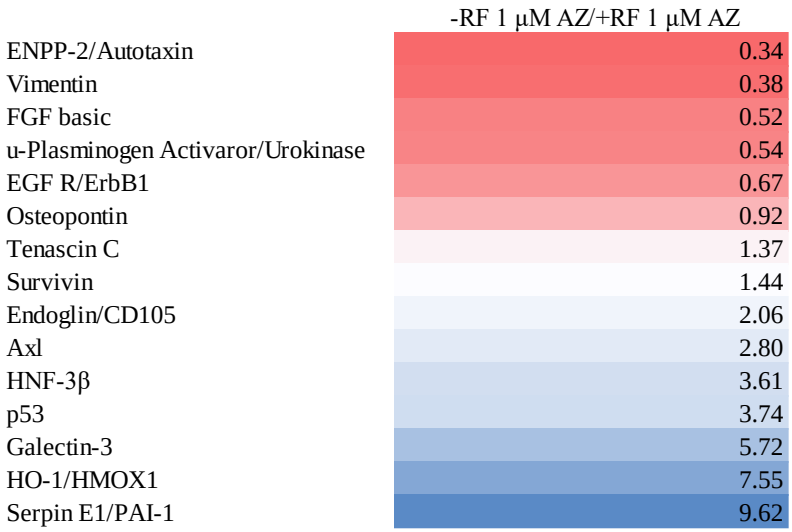

Figure 21. Protein biomarkers comparison between -RF 1 µM AZ/+RF 1 µM AZ.

Conversely, under these stress conditions proteins including ENPP-2/Autotaxin, Vimentin, FGF basic, and u-Plasminogen Activator/Urokinase are downregulated (values below 1, red), therefore indicating lower cell motility, invasiveness, and growth signalling. This trend supports the hypothesis that, in combination with CAIX inhibition, metabolic reprogramming, especially riboflavin depletion, not only strains the cells but also inhibits their capacity to migrate and invade, hence perhaps therapeutally beneficial.

Overall, these proteomic profiles show that CAIX inhibition and metabolic stress simultaneously control important pathways in cancer cells, so balancing life and death, and between migration and adhesion. Together with overexpression of stress response proteins, the observed downregulation

of pro-migratory and anti-apoptotic proteins exposes both weaknesses and adaptive processes that might be taken advantage of for more successful cancer treatment.

3.4. Galactose as another type of cell metabolic reprograming

Additionally, a different type of metabolic cell reprograming was tested, which involved using galactose in cell culture medium. In cells grown with galactose instead of glucose, glycolysis is suppressed and mitochondrial respiration is enhanced. This shift in metabolic pathways allowed for a more precise assessment of mitochondrial function and the impact of CAIX inhibitors under altered metabolic conditions, providing deeper insights into the cellular responses and potential therapeutic implications of metabolic reprogramming

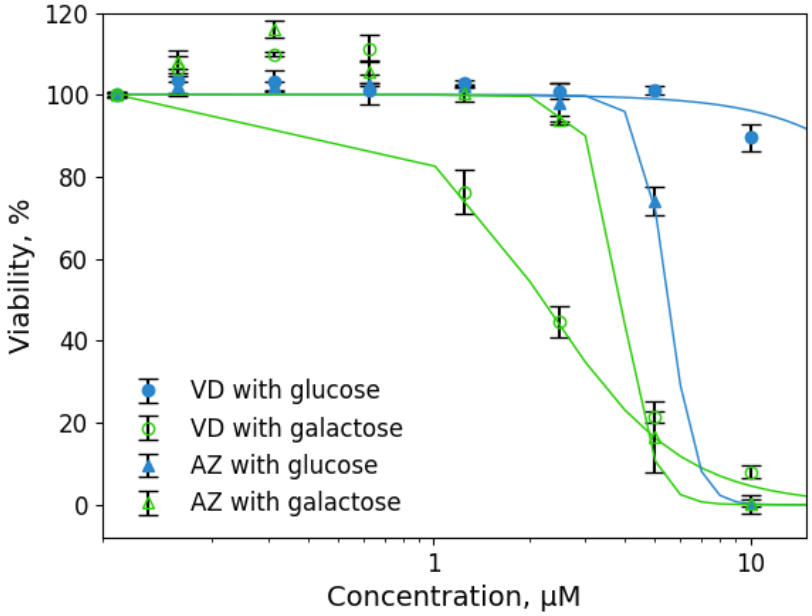

Figure 22. CAIX inhibitor effect on 143B cells viability glucose vs galactose (n=3).

Table 10. CAIX inhibitor LC50 values in 143B cells

CAIX inhibitor	**LC_{50} in live 143B cells, μM**	
	Glucose	Galactose
VD	>10	2.2
AZ	5.5	3.9

The SRB assay was performed to determine the toxicity of the CAIX inhibitor in glucose and galactose media. Significant differences between these conditions could be seen only with the VD inhibitor (Figure 22 and Table 12). With this inhibitor, the lethal dose dropped from more than 10 μM to 2 μM, indicating a much higher toxicity in galactose medium compared to glucose medium. This

suggests that the metabolic environment can significantly impact the efficacy and toxicity of the VD inhibitor. With AZ, the difference in LC_{50} values is not as high, being 5.5 μM in glucose medium and 3.9 μM in galactose medium. This smaller variation indicates that AZ's toxicity is less affected by the metabolic conditions provided by different sugars in cell culture media. These findings highlight the importance of considering the cellular metabolic state when evaluating the toxicity and effectiveness of CAIX inhibitors.

3.5. Knockout of the *CA9* gene in 143B cancer cells using CRISPR/Cas9

CA9 gene knockouts in 143B cancer cells were created with intention to repeat experiments and see how the inhibitor effects correlate with CAIX expression.

Before knocking out the *CA9* gene in 143B cells, finding the optimum transfection method for this cell type was necessary. Several transfection procedures and conditions were tested to see which would be the best. For optimization of the procedure a plasmid for GFP expression was used. The optimization of transfection conditions is critical in this case, because the success of gene knockout clone generation directly depends on the number of transfected CRISPR/Cas9-transfected cells.

First, the transfection by electroporation was tested. On the first day, 143B cells were plated in a T182 flask with fresh medium. The next day, cells were collected, and 2 million cells were resuspended in 400 μl of intracellular buffer per transfection and electroporated at different voltage setting. After electroporation, cells were transferred to a 10 cm cell culture plate, and the medium was changed after 6 hours. On day three, cells were collected, and transfection efficiency was checked using flow cytometry. Different voltages and DNA amounts were combined as specified in Table 7.

Table 7. Conditions and efficiency of electroporation.

Sample	Plasmid	DNA amount, μg	Voltage, V	Efficiency, %
A	1-11 (negative control)	20	220	1.7
B	1-1060/61 (positive control)	10	220	12.7
C	1-1060/61 (positive control)	10	280	22.0
D	1-1060/61 (positive control)	10	310	18.9
E	1-1060/61 (positive control)	20	220	19.5
F	1-1060/61 (positive control)	20	250	15.2

Secondly, PEI transfection was tested. On the first day, 143B cells were plated in a 12-well plate at a density of 7×10^4 cells per well in 1 ml of fresh medium. The next day, the old medium was discarded, and fresh medium along with DNA:PEI mixtures were added to the wells. On day three, all cells were collected, and transfection efficiency was checked using flow cytometry. Different DNA and PEI ratios, as well as DNA amounts, were as specified in Table 8.

Table 8. Conditions and efficiency of PEI transfection

Sample	Plasmid	DNA amount, µg	DNA:PEI ratio	Efficiency, %
A	-	0	1:6	2.1
B	1-1060/61 (positive control)	1	1:6	4.0
C	1-1060/61 (positive control)	3	1:6	27.0
D	1-1060/61 (positive control)	1	1:3	1.8
E	1-1060/61 (positive control)	3	1:3	19.0

PEI transfection using a DNA:PEI ratio of 1:6 and 3 µg of DNA per well (in a 12-well plate) was determined to be the most effective mix for 143B cells. This conclusion was made based on the maximum transfection efficiency of 27.0% among all tested conditions (Tables 7 and 8), as well as the fact that cell viability 24 hours after PEI transfection was higher than viability following electroporation. Furthermore, the PEI transfection method proved to be more cost-effective and easy to scale up for bigger experiments, making it a better option for future gene knockout investigations.

CA9 gene knockout in 143B cells was developed using PEI reagent, described in chapter PEI Transfection. To determine which clone had the *CA9* gene knocked out Western Blot. Judging from the results of Western Blot, there is a high possibility of CAIX gene knockout in clone #3, because a band corresponding to CAIX protein cannot be seen (Figure 23). Results will have to be confirmed by additional mathods, such as flow cytometry and genomic PCR.

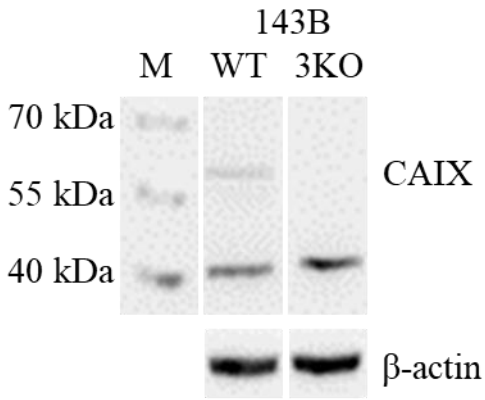

Figure 23. Western Blot of 143B WT cells and CAIX-knockout clone #3 (3KO).

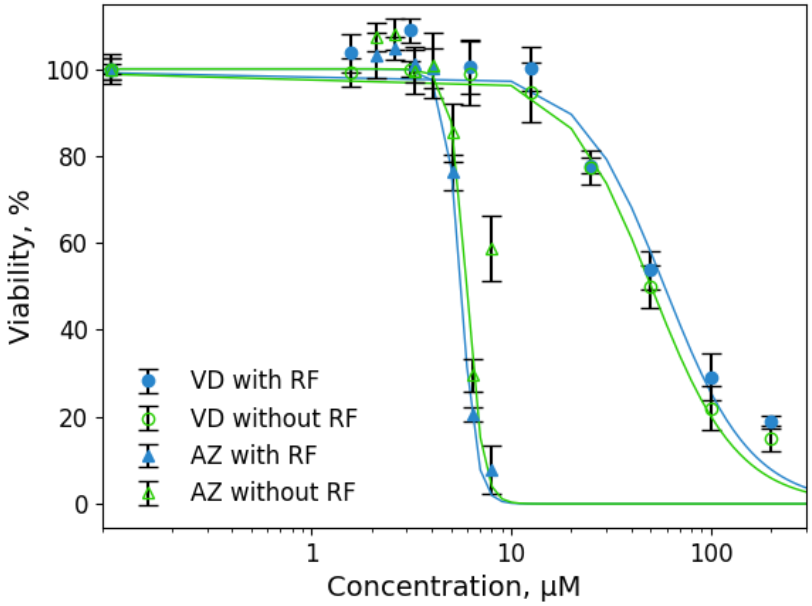

Figure 24. CAIX inhibitor effect on 143B CAIX-knockout clone #3 cells viability ±RF (n=3).

Table 11. . CAIX inhibitor LC_{50} values in 143B CAIX-knockout clone #3 cells

CAIX inhibitor	**LC_{50} in live 143B KO cells, µM**	
	With RF	Without RF
VD	58.6	50.2
AZ	5.4	6

Between the two knockout cells cultivation conditions, with and without RF, significant differences cannot be seen at lethal inhibitor concentrations (Figure 24). Also important to mention, that there is no significant differences in the lethal inhibitor concentrations compared to 143B WT cell (Table 9 and 11). Experimentally determined LC_{50} values were higher for VD. With RF, VD 58.6 µM, AZ 5.4 µM; and without RF, VD 50.2 µM, AZ 6 µM.

4. Discussion

This study investigated the effects of metabolic reprogramming on the sensitivity of 143B osteosarcoma cells to CAIX inhibition, and characterized the resultant changes in oncoprotein expression. The research aimed to elucidate how altering cellular metabolism through RF depletion and galactose substitution conditions affects CAIX expression and the efficacy of CAIX inhibitors (VD11-4-2 and AZ19-3-2).

CAIX expression has been closely associated with hypoxic conditions in tumours, where it is transcriptionally upregulated by HIF-1α to facilitate pH regulation and cell survival. However, our findings, demonstrate that CAIX is also induced by non-hypoxic stressors, specifically RF deprivation and low serum (1% FBS) conditions. This broader induction profile might suggests that CAIX acts as a general responder to environmental and metabolic stress, not solely to oxygen deprivation.

The upregulation of CAIX under RF depletion and low serum conditions may result from the activation of alternative stress pathways, such as nutrient sensing, oxidative stress response, and unfolded protein response, which can converge on the CA9 promoter. While HIF-1α remains a central regulator, other transcription factors may contribute to CAIX induction under these conditions. This expanded regulatory network enhances the tumour's ability to adapt to fluctuating microenvironmental challenges, including nutrient limitation and oxidative stress.

Metabolic reprogramming by RF deprivation impairs mitochondrial function by destabilizing respiratory complexes I and II, further reducing the cell's metabolic flexibility. Meanwhile, substituting glucose with galactose forces cells to rely more heavily on oxidative phosphorylation rather than glycolysis. Our results show that these interventions decrease both glycolytic capacity and mitochondrial spare respiratory capacity, consistent with a more vulnerable metabolic phenotype.

Both VD11-4-2 and AZ19-3-2 CAIX inhibitors reduced cell viability in a dose-dependent manner, although LC_{50} values observed in metabolically reprogrammed and nutrient-stressed cells were similar. But by implementing more sensitive methods like Seahorse and flow cytometry, we observed significantly lower effective inhibitor concentrations. This suggests that limiting metabolic adaptability renders cancer cells more susceptible to disruptions in pH homeostasis mediated by CAIX inhibition. The synergy between metabolic stress and CAIX inhibition may be harnessed therapeutically to overcome resistance mechanisms inherent in highly adaptable tumour cells.

Changes in the expression of oncoproteins are shown by proteomic profiling of 143B osteosarcoma cells under normal riboflavin conditions, with and without CAIX inhibition. Higher expression of Endoglin/CD105, Axl, HNF-3β, Galectin-3, and Serpin E1/PAI-1 in cells not exposed to the CAIX inhibitor. Suggesting that CAIX inhibition reduces paths supporting vascular growth, tissue remodelling, and cellular adaptability. By contrast, Vimentin, FGF basic, and Osteopontin were expressed

at lower levels in normal conditions but were elevated upon CAIX inhibition (red shading), therefore showing an adaptive cellular response to preserve migratory and proliferative capability under metabolic stress. These results taken together show that CAIX inhibition in the presence of riboflavin not only reduces important survival and adhesion pathways but also sets off compensation mechanisms that might improve some facets of cellular adaptability. This dual effect emphasises the complexity of targeting CAIX in metabolically reprogrammed cancer cells and the possibility of combination treatments utilising these adaptive weaknesses.

The redundancy of pH regulation and metabolic pathways in cancer cells poses a challenge for monotherapy approaches. However, our data suggest that simultaneous targeting of multiple adaptive mechanisms such as combining CAIX inhibition with metabolic stress can overcome compensatory resistance and induce cell death more effectively.

While this study provides valuable insights, several limitations should be acknowledged. First, experiments were conducted in vitro using a single osteosarcoma cell line (143B), which may not fully capture the complexity of the tumour microenvironment in vivo. Second, while proteomic analysis identified multiple differentially expressed proteins, functional validation of these candidates was beyond the scope of this work. Third, the use of artificial metabolic stressors (e.g., galactose, RF deprivation) may not perfectly mimic physiological conditions in human tumours.

Future research could include: validation of the observed effects in additional cancer cell lines and primary tumour samples; investigation of the molecular mechanisms underlying stress-induced CAIX expression, including the roles of non-HIF transcription factors; assessment of the efficacy of combined CAIX inhibition and metabolic interventions in animal models and, ultimately, in clinical trial; exploration of the potential for CAIX expression under nutrient stress to serve as a biomarker for therapy selection.

In summary, this study demonstrates that CAIX expression is induced not only by hypoxia but also by nutrient and metabolic stress. Metabolic reprogramming sensitizes osteosarcoma cells to CAIX inhibition, and proteomic analysis reveals widespread changes in energy metabolism and stress response pathways. These findings support a combinatorial therapeutic strategy targeting both metabolic flexibility and pH regulation to overcome tumour resistance and improve cancer treatment outcomes.

Conclusions

1. RF depletion significantly reduced mitochondrial respiration and induced CAIX expression in 143B cancer cells.
2. Both AlamarBlue and SRB assays reported the viability of the whole cells population and not only the fraction that expressed CAIX, which restricted their sensitivity, especially when dealing with lower doses of inhibitors.
3. By focusing on CAIX-positive cells using flow cytometry, it was possible to identify effects on cancer cells at lower concentrations.
4. The Seahorse assay also demonstrated the capacity to detect effects on live cell mitochondrial respiration at lower inhibitor concentrations.
5. Replacing glucose with galactose showed a notable difference in inhibitor LC_{50} concentration, especially for conditions where inhibitor VD11-4-2 was used. This suggests that the metabolic environment can significantly impact the efficacy and toxicity of the inhibitors.
6. Our results highlight the importance of using more precise tests to appropriately assess the metabolic and toxic effects of CAIX inhibitors.

Scientific contributions during Master's studies

Conference presentations:

- **Agnė Kvietkauskaitė**, Jurgita Matulienė. (2024, April 16-17) Effect of Carbonic Anhydrase IX Inhibitors on 2D And 3D Cancer Cell Cultures. Coins 2024. Vilnius, Lithuania (poster presentation)
- **Agnė Kvietkauskaitė**, Jurgita Matulienė, R. Martin Vabulas. (2025, March 17-20) Metabolic Reprograming Using Riboflavin to Induce Synthetic Lethality by CAIX Inhibitors. Coins 2025. Vilnius, Lithuania (poster presentation)

Internship:

- 6-month long internship (from September 2023 till March 2024) Guest Researcher at Charité – Universitätsmedizin Berlin, Institute of Biochemistry. Funded by Erasmus+ program.

Peer-reviewed publications (unrelated to results presented in Master's thesis):

- Petrosiute, A., Zakšauskas, A., Lučiūnaitė, A., Petrauskas, V., Baranauskienė, L., **Kvietkauskaitė, A.**, Ščerbavičienė, A., Tamošiūnaitė, M., Musvicaitė, J., Jankūnaitė, A., Žvinys, G., Stančaitis, L., Čapkauskaitė, E., Mickevičiūtė, A., Juozapaitienė, V., Dudutienė, V., Zubrienė, A., Grincevičienė, Š., Bukelskienė, V., Schiöth, H. B., … Matulis, D. (2025). Carbonic anhydrase IX inhibition as a path to treat neuroblastoma. British journal of pharmacology, 10.1111/bph.17429. Advance online publication. https://doi.org/10.1111/bph.17429
- Aivaras Vaškevičius, Denis Baronas, Janis Leitans, **Agnė Kvietkauskaitė**, Audronė Rukšėnaitė, Elena Manakova, Zigmantas Toleikis, Algirdas Kaupinis, Andris Kazaks, Marius Gedgaudas, Aurelija Mickevičiūtė, Vaida Juozapaitienė, Helgi B Schiöth, Kristaps Jaudzems, Mindaugas Valius, Kaspars Tars, Saulius Gražulis, Franz-Josef Meyer-Almes, Jurgita Matulienė, Asta Zubrienė, Virginija Dudutienė, Daumantas Matulis (2024) Targeted anticancer pre-vinylsulfone covalent inhibitors of carbonic anhydrase IX eLife 13:RP101401 https://doi.org/10.7554/eLife.101401.3

Acknowledgments

I would like to express my deepest gratitude to my supervisor Dr. Jurgita Matulienė and consultant prof. Dr. R. Martin Vabulas for the time they have given me with the training, various experiments planning, and countless corrections of papers and presentations.

I deeply appreciate prof. Dr. Daumantas Matulis for giving me a chance to join his laboratory.

My huge thanks to whole Department of Biothermodynamics and Drug design – Agne Petrosiute for helping with comprehensive training and knowledge in several cell biology techniques; Aurelija Mickevičiūtė for giving me the comprehensive training and knowledge in molecular biology; my sincere thanks to Dr. Vytautas Petrauskas for helping me learn how to use Python; Team of Organic Chemists who synthesized all the compounds; and everyone else for providing friendly work environment.

I give my deep gratitude to prof. Dr. R. Martin Vabulas and his research group for accepting me into her lab there during my stay at Charite and Erasmus+ program for funding my internship.

VILNIAUS UNIVERSITETAS
GYVYBĖS MOKSLŲ CENTRAS

Agnė Kvietkauskaitė

Magistro baigiamasis darbas

Magistro studijų programos baigiamojo darbo pavadinimas

SANTRAUKA

Karbanhidrazė IX (CAIX) yra transmembraninis baltymas, kuris ypač gausiai ekpresuojamas daugelyje kietųjų navikų, kur jis palaiko vėžinių ląstelių išgyvenamumą hipoksijos sąlygomis reguliuodamas pH homeostazę. Nors hipoksija yra pagrindinis CAIX aktyvavimo veiksnis, naujausi tyrimai rodo, kad CAIX raiška gali būti padidinta ir veikiant kitiems ląstelės streso veiksniams, tokiems kaip maisto medžiagų trūkumas (pvz., riboflavino (RF) deficitas) arba maža serumo koncentracija (1% FBS) terpėje. CAIX selektyvus slopinimas yra perspektyvi vėžio terapijos strategija, tačiau vėžinių ląstelių metabolinis plastiškumas dažnai riboja šių inhibitorių veiksmingumą. Šiame darbe tiriama, ar metabolinio reprogramavimo būdai, pakeičiant gliukozės galaktoze bei RF trūkumas, gali padidinti osteosarkomos ląstelių (143B) jautrumą CAIX inhibitoriams, ir apibūdina su tuo susijusius onkobaltymų ekspresijos pokyčius.

143B žmogaus osteosarkomos ląstelės buvo metabolinitiškai perprogramuptos, naudojant RF trūkumą arba galaktozę, po to veiktos CAIX inhibitoriais (VD11-4-2 arba AZ19-3-2). Mitochondrijų respiracija vertintas naudojant „Seahorse XF Cell Mito Stress Test“, o inhibitorių efektas matuotas tekmės citometrija, AlamarBlue ir SRB metodais. CRISPR/Cas9 technologija panaudota sukurti ląsteles su išveiklintu *CA9* genu. Baltymų ekspresijos analizė atlikta identifikuoti onkobaltymų ekspresijos pokyčius, atsirandančius veikiant ląsteles CAIX inhibitoriais ir metaboliniu stresu.

Metabolinis perprogramavimas, sukeliant RF trūkumą, sumažino mitochondrijų kvėpavimo gebą 143B ląstelėse. Abu CAIX inhibitoriai sumažino ląstelių gyvybingumą nuo dozės priklausomu būdu, o didesnis jautrumas buvo stebimas metabolinio streso sąlygomis. Svarbu, kad CAIX išraiška 143B ląstelėse gali būti suaktyvinta ne tik hipoksijos, bet ir RF trūkumo arba mažos serumo koncentracijos. Proteomikos analizė atskleidė reikšmingus baltymų, susijusių su energijos metabolizmu, streso atsaku ir ląstelės išgyvenimo keliais, pokyčius po CAIX slopinimo. Šie rezultatai patvirtina, kad metabolinio perprogramavimo ir CAIX inhibitorių derinys gali būti efektyvi vėžio terapijos strategija.

VILNIUS UNIVERSITY
LIFE SCIENCES CENTER

Agnė Kvietkauskaitė

Master's thesis

Metabolic Reprograming of Cancer Cells Using Riboflavin to Induce Synthetic Lethality by CAIX Inhibitors

ABSTRACT

Carbonic anhydrase IX (CAIX) is a transmembrane enzyme overexpressed in many solid tumours, where it supports cancer cell survival under hypoxic conditions by regulating pH homeostasis. While hypoxia is a well-established inducer of CAIX via HIF-1α, recent evidence suggests that CAIX expression can also be upregulated by other cellular stresses, including nutrient deprivation such as riboflavin (RF) depletion and culture in low serum (1% FBS). Selective inhibition of CAIX is a promising strategy for cancer therapy, but the metabolic plasticity of cancer cells often limits the efficacy of such inhibitors. This study investigates whether metabolic reprogramming via manipulation of glucose and galactose availability and RF deprivation can sensitize osteosarcoma cells (143B) to CAIX inhibition, and characterizes the resulting proteomic changes.

143B human osteosarcoma cells were subjected to metabolic reprogramming using RF deprivation or galactose, then treated with two CAIX inhibitors (VD11-4-2 and AZ19-3-2). Mitochondrial respiration was assessed using the Seahorse XF Cell Mito Stress Test, while inhibitor effects were evaluated by flow cytometry, AlamarBlue and SRB assays. CRISPR/Cas9 system was used to generate knockout *CA9* gene cell lines. Protein profiling was conducted to identify oncoprotein expression changes in response to CAIX inhibition and metabolic stress.

Metabolic reprogramming by RF deprivation reduced mitochondrial respiratory capacity in 143B cells. Both CAIX inhibitors decreased cell viability in a dose-dependent manner, with enhanced sensitivity observed under metabolic stress conditions. Notably, CAIX expression in 143B cells can be induced not only by hypoxia but also by RF depletion and low serum concentration, highlighting the CAIX role as a cellular stress responder. Proteomic profiling revealed significant alterations in proteins related to energy metabolism, stress response, and cell survival pathways following CAIX inhibition. These findings support the combined use of metabolic interventions and CAIX inhibitors as a therapeutic strategy in cancer.

References

Alterio, V., Hilvo, M., di Fiore, A., Supuran, C. T., Pan, P., Parkkila, S., Scaloni, A., Pastorek, J., Pastorekova, S., Pedone, C., Scozzafava, A., Monti, S. M., & de Simone, G. (2009). Crystal structure of the catalytic domain of the tumor-associated human carbonic anhydrase IX. Proceedings of the National Academy of Sciences, 106(38), 16233–16238. https://doi.org/10.1073/pnas.0908301106

Angeli, A., Carta, F., & Supuran, C. T. (2020). Carbonic Anhydrases: Versatile and Useful Biocatalysts in Chemistry and Biochemistry. Catalysts, 10(9), 1008. https://doi.org/10.3390/catal10091008

Baranauskienė, L., & Matulis, D. (2019a). Overview of Human Carbonic Anhydrases. In D. Matulis (Ed.), Carbonic Anhydrase as Drug Target (pp. 3–14). Springer International Publishing. https://doi.org/10.1007/978-3-030-12780-0_1

Baranauskienė, L., & Matulis, D. (2019b). Catalytic Activity and Inhibition of Human Carbonic Anhydrases. In Carbonic Anhydrase as Drug Target (pp. 39–49). Springer International Publishing. https://doi.org/10.1007/978-3-030-12780-0_3

Becker, H. M. (2020). Carbonic anhydrase IX and acid transport in cancer. British Journal of Cancer, 122(2), 157–167. https://doi.org/10.1038/s41416-019-0642-z

Becker, H. M., & Deitmer, J. W. (2020). Transport Metabolons and Acid/Base Balance in Tumor Cells. Cancers, 12(4), 899. https://doi.org/10.3390/cancers12040899

Carta, F., Vullo, D., & Angeli, A. (2021). Design, synthesis, and biological evaluation of selective hCA IX inhibitors. In pH-Interfering Agents as Chemosensitizers in Cancer Therapy (pp. 63–78). Elsevier. https://doi.org/10.1016/B978-0-12-820701-7.00014-2

Chegwidden, W.R. (2021). The Carbonic Anhydrases in Health and Disease. In: Chegwidden, W.R., Carter, N.D. (eds) The Carbonic Anhydrases: Current and Emerging Therapeutic Targets. Progress in Drug Research, vol 75. Springer, Cham. https://doi.org/10.1007/978-3-030-79511-5_1

Ciccone, L., Cerri, C., Nencetti, S., & Orlandini, E. (2021). Carbonic Anhydrase Inhibitors and Epilepsy: State of the Art and Future Perspectives. Molecules, 26(21), 6380. https://doi.org/10.3390/molecules26216380

Conte, F., van Buuringen, N., Voermans, N. C., & Lefeber, D. J. (2021). Galactose in human metabolism, glycosylation and congenital metabolic diseases: Time for a closer look. Biochimica et Biophysica Acta (BBA) - General Subjects, 1865(8), 129898. https://doi.org/10.1016/j.bbagen.2021.129898

di Fiore, A., Monti, D. M., Scaloni, A., de Simone, G., & Monti, S. M. (2018). Protective Role of Carbonic Anhydrases III and VII in Cellular Defense Mechanisms upon Redox Unbalance. Oxidative Medicine and Cellular Longevity, 2018, 1–9. https://doi.org/10.1155/2018/2018306

Dudutiene, V., Matuliene, J., Smirnov, A., Timm, D. D., Zubriene, A., Baranauskiene, L., Morkunaite, V., Smirnoviene, J., Michailoviene, V., Juozapaitiene, V., Mickevičiute, A., Kazokaite, J., Bakšyte, S., Kasiliauskaite, A., Jachno, J., Revuckiene, J., Kišonaite, M., Pilipuityte, V., Ivanauskaite, E., … Matulis, D. (2014). Discovery and characterization of novel selective inhibitors of carbonic anhydrase IX. Journal of Medicinal Chemistry, 57(22), 9435–9446. https://doi.org/10.1021/JM501003K/SUPPL_FILE/JM501003K_SI_001.PDF

Holden, H. M., Rayment, I., & Thoden, J. B. (2003). Structure and Function of Enzymes of the Leloir Pathway for Galactose Metabolism. Journal of Biological Chemistry, 278(45), 43885–43888. https://doi.org/10.1074/jbc.r300025200

Jensen, E. L., Clement, R., Kosta, A., Maberly, S. C., & Gontero, B. (2019). A new widespread subclass of carbonic anhydrase in marine phytoplankton. The ISME Journal, 13(8), 2094–2106. https://doi.org/10.1038/s41396-019-0426-8

Kamiloglu, S., Sari, G., Ozdal, T., & Capanoglu, E. (2020). Guidelines for cell viability assays. Food Frontiers, 1(3), 332–349. https://doi.org/10.1002/fft2.44

Koltai, T., Reshkin, S. J., & Harguindey, S. (2020). Carbonic anhydrases. In An Innovative Approach to Understanding and Treating Cancer: Targeting pH (pp. 157–176). Elsevier. https://doi.org/10.1016/B978-0-12-819059-3.00007-1

Lee, S.-H., McIntyre, D., Honess, D., Hulikova, A., Pacheco-Torres, J., Cerdán, S., Swietach, P., Harris, A. L., & Griffiths, J. R. (2018). Carbonic anhydrase IX is a pH-stat that sets an acidic tumour extracellular pH in vivo. British Journal of Cancer, 119(5), 622–630. https://doi.org/10.1038/s41416-018-0216-5

Linkuvienė, V., Zubrienė, A., Manakova, E., Petrauskas, V., Baranauskienė, L., Zakšauskas, A., Smirnov, A., Gražulis, S., Ladbury, J. E., & Matulis, D. (2018). Thermodynamic, kinetic, and structural parameterization of human carbonic anhydrase interactions toward enhanced inhibitor design. Quarterly Reviews of Biophysics, 51, e10. https://doi.org/10.1017/S0033583518000082

Liu, S.; Hu, W.; Wang, Z.; Chen, T. Production of riboflavin and related cofactors by biotechnological processes. Microb. Cell Factories 2020, 19, 31.

Maren, T. H. (1987). Carbonic anhydrase: General perspective and advances in glaucoma research. Drug Development Research, 10(4), 255–276. https://doi.org/10.1002/ddr.430100407

McDonald, P. C., Chia, S., Bedard, P. L., Chu, Q., Lyle, M., Tang, L., Singh, M., Zhang, Z., Supuran, C. T., Renouf, D. J., & Dedhar, S. (2020). A Phase 1 Study of SLC-0111, a Novel Inhibitor of Carbonic Anhydrase IX, in Patients With Advanced Solid Tumors. American Journal of Clinical Oncology, 43(7), 484–490. https://doi.org/10.1097/COC.0000000000000691

Navarro, C., Ortega, Á., Santeliz, R., Garrido, B., Chacín, M., Galban, N., Vera, I., De Sanctis, J. B., & Bermúdez, V. (2022). Metabolic reprogramming in cancer cells: Emerging molecular mechanisms and novel therapeutic approaches. Pharmaceutics, 14(6), 1303. https://doi.org/10.3390/pharmaceutics14061303

Nisco, A., Tolomeo, M., Scalise, M., Zanier, K., & Barile, M. (2024). Exploring the impact of flavin homeostasis on Cancer Cell metabolism. Biochimica et Biophysica Acta (BBA) - Reviews on Cancer, 1879(5), 189149. https://doi.org/10.1016/j.bbcan.2024.189149

Nocentini, A., Supuran, C. T., & Capasso, C. (2021). An overview on the recently discovered iota-carbonic anhydrases. Journal of Enzyme Inhibition and Medicinal Chemistry, 36(1), 1988–1995. https://doi.org/10.1080/14756366.2021.1972995

Pastorek, J., Pastoreková, S., Callebaut, I., Mornon, J. P., Zelník, V., Opavský, R., Zat'ovicová, M., Liao, S., Portetelle, D., & Stanbridge, E. J. (1994). Cloning and characterization of MN, a human tumor-associated protein with a domain homologous to carbonic anhydrase and a putative helix-loop-helix DNA binding segment. Oncogene, 9(10), 2877–2888.

Pastorekova, S., & Gillies, R. J. (2019). The role of carbonic anhydrase IX in cancer development: links to hypoxia, acidosis, and beyond. Cancer and Metastasis Reviews, 38(1–2), 65–77. https://doi.org/10.1007/s10555-019-09799-0

Pastoreková, S., Závadová, Z., Košťál, M., Babušíková, O., & Závada, J. (1992). A novel quasi-viral agent, MaTu, is a two-component system. Virology, 187(2), 620–626. https://doi.org/10.1016/0042-6822(92)90464-Z

Piccinini, F. (2015). AnaSP: A software suite for automatic image analysis of multicellular spheroids. Computer Methods and Programs in Biomedicine, 119(1), 43–52. https://doi.org/10.1016/j.cmpb.2015.02.006

Queen, A., Bhutto, H. N., Yousuf, M., Syed, M. A., & Hassan, Md. I. (2022). Carbonic anhydrase IX: A tumor acidification switch in heterogeneity and chemokine regulation. Seminars in Cancer Biology, 86, 899–913. https://doi.org/10.1016/j.semcancer.2022.01.001

Shaikh, A. B., Fang, H., Li, M., Chen, S., Shang, P., & Shang, X. (2020). Reduced expression of carbonic anhydrase III in skeletal muscles could be linked to muscle fatigue: A rat muscle fatigue model. Journal of Orthopaedic Translation, 22, 116–123. https://doi.org/10.1016/j.jot.2019.08.008

Silverman, D. N., & Lindskog, S. (1988). The catalytic mechanism of carbonic anhydrase: implications of a rate-limiting protolysis of water. Accounts of Chemical Research, 21(1), 30–36. https://doi.org/10.1021/ar00145a005

Smirnovienė, J., Smirnov, A., Zakšauskas, A., Zubrienė, A., Petrauskas, V., Mickevičiūtė, A., Michailovienė, V., Čapkauskaitė, E., Manakova, E., Gražulis, S., Baranauskienė, L., Chen, W., Ladbury, J. E., & Matulis, D. (2021). Switching the Inhibitor-Enzyme Recognition Profile via Chimeric Carbonic Anhydrase XII. ChemistryOpen, 10(5), 567–580. https://doi.org/10.1002/open.202100042

Stoner, A., Harris, A., Oddone, F., Belamkar, A., Verticchio Vercellin, A. C., Shin, J., Januleviciene, I., & Siesky, B. (2022). Topical carbonic anhydrase inhibitors and glaucoma in 2021: where do we stand? British Journal of Ophthalmology, 106(10), 1332–1337. https://doi.org/10.1136/bjophthalmol-2021-319530

Sun, H., Chen, L., Cao, S., Liang, Y., & Xu, Y. (2019). Warburg Effects in Cancer and Normal Proliferating Cells: Two Tales of the Same Name. Genomics, proteomics & bioinformatics, 17(3), 273–286. https://doi.org/10.1016/j.gpb.2018.12.006

Supuran, C. T. (2021). Emerging role of carbonic anhydrase inhibitors. Clinical Science, 135(10), 1233–1249. https://doi.org/10.1042/CS20210040

Supuran, C. T. (2022). Anti-obesity carbonic anhydrase inhibitors: challenges and opportunities. Journal of Enzyme Inhibition and Medicinal Chemistry, 37(1), 2478–2488. https://doi.org/10.1080/14756366.2022.2121393

Tars, K., & Matulis, D. (2019). X-Ray Crystallographic Structures of High-Affinity and High-Selectivity Inhibitor Complexes with CA IX That Plays a Special Role in Cancer. In D. Matulis (Ed.), Carbonic Anhydrase as Drug Target (pp. 203–213). Springer International Publishing. https://doi.org/10.1007/978-3-030-12780-0_14

Warburg O. (1956). On the origin of cancer cells. Science (New York, N.Y.), 123(3191), 309–314. https://doi.org/10.1126/science.123.3191.309

Zakšauskas, A., Čapkauskaitė, E., Paketurytė-Latvė, V., Smirnov, A., Leitans, J., Kazaks, A., Dvinskis, E., Stančaitis, L., Mickevičiūtė, A., Jachno, J., Jezepčikas, L., Linkuvienė, V., Sakalauskas, A., Manakova, E., Gražulis, S., Matulienė, J., Tars, K., & Matulis, D. (2021). Methyl 2-Halo-4-Substituted-5-Sulfamoyl-Benzoates as High Affinity and Selective Inhibitors of Carbonic Anhydrase IX. International Journal of Molecular Sciences, 23(1), 130. https://doi.org/10.3390/ijms23010130

Zamanova, S., Shabana, A. M., Mondal, U. K., & Ilies, M. A. (2019). Carbonic anhydrases as disease markers. Expert Opinion on Therapeutic Patents, 29(7), 509–533. https://doi.org/10.1080/13543776.2019.1629419

Zavala-Tecuapetla, C., Cuellar-Herrera, M., & Luna-Munguia, H. (2020). Insights into Potential Targets for Therapeutic Intervention in Epilepsy. International Journal of Molecular Sciences, 21(22), 8573. https://doi.org/10.3390/ijms21228573